

Supporting Information

Dizinc Lactide Polymerization Catalysts: Hyperactivity by Control of Ligand Conformation and Metallic Cooperativity

Arnaud Thevenon, Charles Romain, Michael S. Bennington, Andrew J. P. White, Hannah J. Davidson, Sally Brooker, and Charlotte K. Williams**

anie_201602930_sm_miscellaneous_information.pdf

Supporting Information

Contents

Experimental part:	5
Figure S1: ^1H NMR of HL ^{Open} in CDCl_3 (298 K).....	7
Figure S2: ^1H NMR of 1 (d_8 -THF, 193 K).....	9
Figure S3: ^{13}C NMR of 1 (d_8 -THF, 193 K).....	10
Figure S4: Molecular structure of 1	10
Figure S5: Molecular structure of 1b	11
Figure S6: ^1H NMR of 2 (d_8 -THF, 298 K).....	12
Figure S7: ^{13}C NMR of 2 (d_8 -THF, 298 K).....	12
Figure S8: Molecular structure of 2	13
Figure S9: ^1H NMR of 3 (C_6D_6 , 298 K)	14
Figure S10: ^{13}C NMR of 3 (C_6D_6 , 298 K)	14
Figure S11: Molecular structure of 3	15
Figure S12: ^1H NMR spectra for the kinetic study of the ROP of 1000 eq. of rac-LA using 1	15
Figure S13: Plot of the molecular weight vs the conversion for 1 with 1000 equivalents of rac-LA.	16
Figure S14: Overlap of SEC traces for 1 during the polymerization of 1000 equivalents of rac-LA.....	16
Figure S15: ^1H NMR spectra for the kinetic study of the the ROP of 1000 eq. of rac-LA using 2	16
Figure S16: Plot of the molecular weight vs the conversion for 2 with 1000 equivalents of rac-LA.	17
Figure S17: Overlap of SEC traces for 2 during the polymerization of 1000 equivalents of rac-LA.....	17
Figure S18: ^1H NMR spectra for the kinetic study of the ROP of 1000 eq. of rac-LA using 3	17
Figure S19: Plot of the molecular weight vs conversion for 3 with 1000 equivalents of rac-LA.	18
Figure S20: Overlap of SEC traces for 3 during the polymerization of 1000 equivalents of rac-LA.....	18
Figure S21: MALDI-ToF spectrum obtained for monitoring a polymerization reaction with 1 , 2 or 3 . 19	
Figure S22: Overlaid of ^1H NMR of the reaction of 1 with 2 eq. of IPA (d_8 -THF, 298 K).	19
Figure S23: Overlaid of ^1H NMR of the reaction of 2 with 2 eq. if IPA (d_8 -THF, 298 K).....	20
Figure S24: Overlaid of ^1H NMR of the reaction of 3 with 1 eq. if IPA (d_8 -THF, 298 K).....	20
Table S1: Data of the rac-LA polymerization using 1 , 2 , 3 , 4 , 5 and 6	21
Figure S25: ^1H NMR spectra for the kinetic study of the polymerization: 1000 eq. of rac-LA using 4 . 22	
Figure S26: Plot of $\ln([\text{LA}_0]/[\text{LA}_t])$ vs time for 4 with 1000 equivalents of rac-LA.	22
Figure S27: Plot of the molecular weight vs the conversion for 4 with 1000 equivalents of rac-LA.	23
Figure S28: Overlap of SEC traces for 4 during the polymerization of 1000 equivalents of rac-LA.....	23
Figure S29: ^1H NMR spectra for the kinetic study of the ROP of 1000 eq. of rac-LA using 5	23

Figure S30: ^1H NMR spectra for the kinetic study of the ROP of 1000 eq. of rac-LA using 6	24
Figure S31: Plot of $\ln([LA_0]/[LA_t])$ vs time for 5 and 6 with 1000 equivalents of rac-LA.	24
Figure S32: Plot of the molecular weight vs the conversion for 5 with 1000 equivalents of rac-LA. ...	24
Figure S33: Overlap of SEC traces for 5 during the polymerization of 1000 equivalents of rac-LA.....	25
Figure S34: Plot of the molecular weight vs the conversion for 6 with 1000 equivalents of rac-LA. ...	25
Figure S35: Overlap of SEC traces for 6 during the polymerization of 1000 equivalents of rac-LA.....	25
Figure S36: MALDI-ToF spectrum obtained for a polymerization reaction using alkoxide catalyst.	26
Figure S37: Stack of ^1H NMR spectra for the kinetic study of the ROP of 1000 eq. of rac-LA using 1 in presence of 10 eq. of IPA.	26
Figure S38: Stack of ^1H NMR spectra for the kinetic study of the ROP of 1000 eq. of rac-LA using 2 in presence of 10 eq. of IPA.	27
Figure S39: Stack of ^1H NMR spectra for the kinetic study of the ROP of 1000 eq. of rac-LA using 3 in presence of 10 eq. of IPA.	27
Figure S40: Plot of the molecular weight vs the conversion for 1 under immortal condition with 1000 equivalents of rac-LA and 10 equivalents of IPA.	28
Figure S41: Overlap of SEC traces for 1 during the polymerization of 1000 equivalents of rac-LA under immortal condition (10 eq. of IPA).	28
Figure S42: Plot of the molecular weight vs the conversion for 2 under immortal condition with 1000 equivalents of rac-LA and 10 equivalents of IPA.	29
Figure S43: Overlap of SEC traces for 2 during the polymerization of 1000 equivalents of rac-LA under immortal condition (10 eq. of IPA).	29
Figure S44: Plot of the molecular weight vs the conversion for 3 under immortal condition with 1000 equivalents of rac-LA and 10 equivalents of IPA.	29
Figure S45: Overlap of SEC traces for 3 during the polymerization of 1000 equivalents of rac-LA under immortal condition (10 eq. of IPA).	30
Figure S46: MALDI-ToF spectrum obtained for immortal polymerization reaction for 1 , 2 or 3	30
Figure S47: ^1H NMR spectrum corresponding to the entry 1 in table 1; ROP of 5000 eq. of rac-LA using 1	31
Figure S48: ^1H NMR spectrum corresponding to the entry 2 in table 1	31
Figure S49: Stack of ^1H NMR spectra for the kinetic study of the ROP of 5000 eq. of rac-LA using 1 in presence of 10 eq. of IPA.	32
Figure S50: Stack of ^1H NMR spectra for the kinetic study of the ROP of 5000 eq. of rac-LA using 2 in presence of 10 eq. of IPA.	32
Figure S51: ^1H NMR spectrum corresponding to the entry 5 in table 1; ROP of 5000 eq. of rac-LA using 3 in presence of 10 eq of IPA.....	33
Figure S52: Stack of ^1H NMR spectra for the kinetic study of the ROP of 10,000 eq. of rac-LA using 1 in presence of 20 eq. of IPA.	33
Figure S53: Stack of ^1H NMR spectra for the kinetic study of the ROP of 10,000 eq. of rac-LA using 2 in presence of 20 eq. of IPA.	34

Figure S54: ^1H NMR spectrum corresponding to the entry 8 in table 1; polymerization of 20,000 eq. of rac-LA using 1 in presence of 40 eq of IPA.	34
Figure S55: Stack of ^1H NMR spectra for the kinetic study of the polymerization of 20,000 eq. of rac-LA using 2 in presence of 40 eq. of IPA.....	35
Figure S56: ^1H NMR spectra for the kinetic study of the polymerization of 50,000 eq. of rac-LA using 2 in presence of 50 eq. of IPA..	35
Figure S57: ^1H NMR of 3 (C_6D_6 , 298 K) after 1h of reaction with 2 eq. of IPA	36
Figure S58: Plot of the molecular weight vs the conversion for 2 with 5000 equivalents of rac-LA.	36
Figure S59: Plot of $\ln([\text{LA}_0]/[\text{LA}_t])$ vs time for 1 and 2 at 25 °C under immortal condition with 5000 equivalents of rac-LA and 10 equivalents of IPA.	37
Figure S60: Plot of the molecular weight vs the conversion for 1 under immortal condition with 5000 equivalents of rac-LA and 10 equivalents of IPA.	37
Figure S61: Overlap of SEC traces for 1 during the polymerization of 5000 equivalents of rac-LA under immortal condition (10 eq. of IPA).	37
Figure S62: Plot of the molecular weight vs the conversion for 2 under immortal condition with 5000 equivalents of rac-LA and 10 equivalents of IPA.	38
Figure S63: Overlap of SEC traces for 2 during the polymerization of 5000 equivalents of rac-LA under immortal condition (10 eq. of IPA).	38
Figure S64: Plot of conversion vs time for 1 at 25 °C under immortal condition with 10,000 equivalents of rac-LA and 20 equivalents of IPA.	38
Figure S65: Plot of the molecular weight vs the conversion for 1 under immortal condition with 10,000 equivalents of rac-LA and 20 equivalents of IPA.	39
Figure S66: Overlap of SEC traces for 1 during the polymerization of 10000 equivalents of rac-LA under immortal condition (20 eq. of IPA).....	39
Figure S67: Plot of $\ln([\text{LA}_0]/[\text{LA}_t])$ vs time for 2 , immortal condition, 10,000 equivalents of rac-LA....	40
Figure S68: Plot of the molecular weight vs the conversion for 2 under immortal condition with 10,000 equivalents of rac-LA and 20 equivalents of IPA.	40
Figure S69: Overlap of SEC traces for 2 during the polymerization of 10000 equivalents of rac-LA under immortal condition (20 eq. of IPA).....	40
Figure S70: Plot of $\ln([\text{LA}_0]/[\text{LA}_t])$ vs time for 2 immortal condition, 20,000 equivalents of rac-LA.	41
Figure S71: Plot of the molecular weight vs the conversion for 2 under immortal condition with 20,000 equivalents of rac-LA and 40 equivalents of IPA.	41
Figure S72: Overlap of SEC traces for 2 during the polymerization of 20000 equivalents of rac-LA under immortal condition (40 eq. of IPA).....	42
Figure S73: Plot of $\ln([\text{LA}_0]/[\text{LA}_t])$ vs time for 2 at 25 °C under immortal condition with 50,000 equivalents of rac-LA and 50 equivalents of IPA..	42
Figure S74: Plot of the molecular weight vs the conversion for 2 under immortal condition with 50,000 equivalents of rac-LA and 50 equivalents of IPA.	42
Figure S75: Overlap of SEC traces for 2 during the polymerization of 50000 equivalents of rac-LA under immortal condition (50 eq. of IPA).....	43

Figure S76: ROSSY spectrum of 1 (d ₈ -THF, 193 K).....	43
Figure S77: Overlaid of ¹ H NMR spectrum of 1 from 193 K to 333 K with Δt = 10 K (d ₈ -THF)	44
Figure S78: Proposed dynamic process where two folded conformer of 1 are in equilibrium.	44
Figure S79: Representation of the non-covalent interaction surface in 1	45
Figure S80: Other less favourable equilibrium.	45
Figure S81: Molecular structure of 4	46
Figure S82: ¹ H NMR spectrum of 4 in d ₈ -THF (T = 298 K).....	46
Figure S83: Overlaid of ¹ H NMR spectra of the reaction of 1 with two equivalents of IPA in d ₈ -THF ..	47
Figure S84: Stack of ¹ H NMR spectra for the kinetic study of the polymerization of 1,000 + 200 eq. of rac-LA using 1 in presence of 10 eq. of IPA.....	48
Figure S85: Plot of the conversion of rac-LA vs time for 1 at 25 °C under immortal condition with 1,000 equivalents of rac-LA and 10 equivalents of IPA.	49
Figure S86: Plot of the molecular weight vs the conversion for 1 under immortal condition with 1000 equivalents of rac-LA and 10 equivalents of IPA.	49
Figure S87: Plot of the conversion of rac-LA vs time for 1 at 25 °C after the addition of 200 eq extra rac-LA monomers to a solution of 1 after full conversion of 1000 eq. of rac-LA.....	50
Figure S88: Plot of the molecular weight vs the conversion for 1 under immortal condition with 1000+200 equivalents of rac-LA and 10 equivalents of IPA.	50
Figure S89: Overlap of SEC traces for 1 during the polymerization of 1000 +200 equivalents of rac-LA under immortal condition (10 eq. of IPA).....	51
Figure S90: Proposed mechanism for the reaction of two equivalents of IPA on 1	51
Figure S91: IRC calculations showing interconversion between two aromatic units	51
Table S2: Data for the DFT calculations as illustrated in Figure S91.....	51
Figure S92: Typical example of a ¹ H { ¹ H} homo nuclear decoupled NMR spectrum of PLA.	52
Calculation of the portion of active catalyst in the case HMDS catalysts.....	52
References	53

Experimental part:

All solvents and reagents were obtained from commercial sources (Aldrich and Merck) and used as received unless stated otherwise. MeCN was dried using a Pure Solv MD-6 Solvent Purification System. Toluene and hexane solvents were pre-dried over potassium hydroxide then refluxed over sodium/benzophenone. THF was dried by storage over molecular sieves after being refluxed over sodium/benzophenone. Isopropanol was dried over calcium hydride, distilled and stored over molecular sieves under inert atmosphere. All dry solvents and reagents were stored under nitrogen and degassed by several freeze-pump-thaw cycles. When stated, manipulations were performed using a double-manifold Schlenk vacuum line under nitrogen atmosphere or a nitrogen-filled glovebox. Rac-LA were recrystallized two times from toluene under inert atmosphere followed by sublimation at 80 °C under reduced pressure. Zinc bis[bis(trimethylsilyl)amide] [$\text{Zn}(\text{HMDS})_2$] were prepared as described previously.¹

NMR: ^1H NMR spectra of the ligands were obtained by MSB on a Varian 400-MR NMR spectrometer at 298 K. ^1H , ^{13}C and 2D NMR (COSY, HMQC) spectra of the complexes were recorded using a Bruker AV 400 MHz spectrometer at 298 K.

ESI-MS: ESI-MS spectra were collected by Jenny Pentelow (Otago) on a Bruker MicrOTOFQ mass spectrometer.

MALDI-TOF MS: MALDI ToF analysis was carried out on Micromass MALDI micro MX spectrometer. The matrix used was the dithranol and potassium trifluoro acetate was used as an additive, when necessary. The samples were prepared as followed: 10 mg/mL THF solutions of the complex, matrix and additive were separately prepared. Then, 20 μL of the complex and 20 μL of the matrix solution were mixed, along with 10 μL of the additive solution, if required. This mixture (2 μL) was then spotted on the MALDI plate and allowed to dry.

X-ray diffraction: Data were collected using an Agilent Xcalibur X 3E diffractometer, and the structures were refined using the SHELXTL and SHELX-2013 program systems. The crystallographic data table of all the compounds can be found in the supporting information (Table S4).

Elemental analysis: For all the ligands, elemental analyses (CHN) were carried out by Campbell Microanalytical Laboratory at the University of Otago, with a standard error of $\pm 0.3\%$. Elemental analysis for all the complexes were determined by Stephen Boyer at London Metropolitan University.

SEC: Two Mixed Bed PSS SDV linear S columns were used in series, with THF as the eluent, at a flow rate of 1 mL/min, on a Shimadzu LC-20AD instrument at 40 °C. Polymer molecular weight

(M_n) was determined by comparison against polystyrene standards. The polymer samples were dissolved in SEC grade THF and filtered prior to analysis.

Computational Details: All calculations were performed using the Gaussian 09 suite of codes (revision C.01). Calculations were carried out at the DFT level of theory, using hybrid functional ω B97XD. All atoms, including zinc, have been described with a 6-31G(d,p) basis set. Geometry optimizations were carried out without any symmetry restrictions. Conductor-like polarizable continuum model (CPCM) was used with THF as the solvent to model solvation. The nature of the extrema was verified with analytical frequency calculations: the stationary points (minima) do not feature imaginary modes, and all transition states reveal precisely one imaginary mode corresponding to the intended reaction. For **IITS**, an IRC calculation was performed which also confirmed the identity of the transition state. Data available at <https://doi.org/10.14469/hpc/430>

Ligand synthesis:

The metal-free Schiff base macrocycles, **H₂L^{Et}** and **H₂L^{Pr}** were prepared as described previously.²

The open (non-cyclic) ligand analogue, **HL^{Open}**, was prepared as follows:

To a yellow refluxing dry MeCN (20 mL) solution of 2,2'-iminobisbenzaldehyde³ (500.9 mg, 2.224 mmol) was added a dry MeCN (25 mL) solution of isobutylamine (0.8 mL, 8mmol). The resulting pale yellow solution was refluxed for a further 150 minutes, before cooling to RT and taking it to dryness *in vacuo*, giving an orange oil. Analysis of the ¹H NMR spectrum indicated some free aldehyde was still present, so the oil was taken up in dry MeCN (25 mL) and the orange solution brought to reflux before adding a dry MeCN (20mL) solution of isobutylamine (0.8 mL, 8mmol). After refluxing for a further hour the solution was left to cool then taken to dryness *in vacuo* giving **HL^{Open}** as an orange-brown oil (572.4 mg, 1.706 mmol, 77%). Found: C, 78.69; H, 8.86; N, 12.65 %. Calculated for C₂₂H₂₉N₃ (335.50 g mol⁻¹): C, 78.76; H, 8.71; N, 12.53 %. ESI(+)-MS (*m/z*): 336.2405 (calc. for [C₂₂H₃₀N₃]⁺ = 336.2434); 358.2220 (calc. for [C₂₂H₂₉N₃Na]⁺ = 358.2254). ¹H NMR (400 MHz, CDCl₃, 298 K) δ (ppm) = 11.33 (br. s, 1H, NH), 8.44 (s, 2H, H7), 7.66 (d, J = 7.57 Hz, 2H, H3), 7.26 (m, 4H, H5/6), 6.95 (m, 2H, H4), 3.40 (dd, J = 6.6, 1.2 Hz, 4H, H8), 1.97 (t sep, J = 6.6, 6.7 Hz, 2H, H9), 0.95 (d, J = 6.7 Hz, 12H, H10). ¹³C NMR (101 MHz, Chloroform-d) δ (ppm) = 161.1 (C=N), 143.8 (*o*-Ph), 131.0 (*m*-Ph), 130.9 (*o*-Ph), 124.4 (*i*-Ph), 120.6 (*p*-Ph), 118.5 (*o*-Ph), 69.9 (N-CH₂-CH), 29.9 (CH-(CH₃)₂), 20.8 ((CH₃)₂-CH).

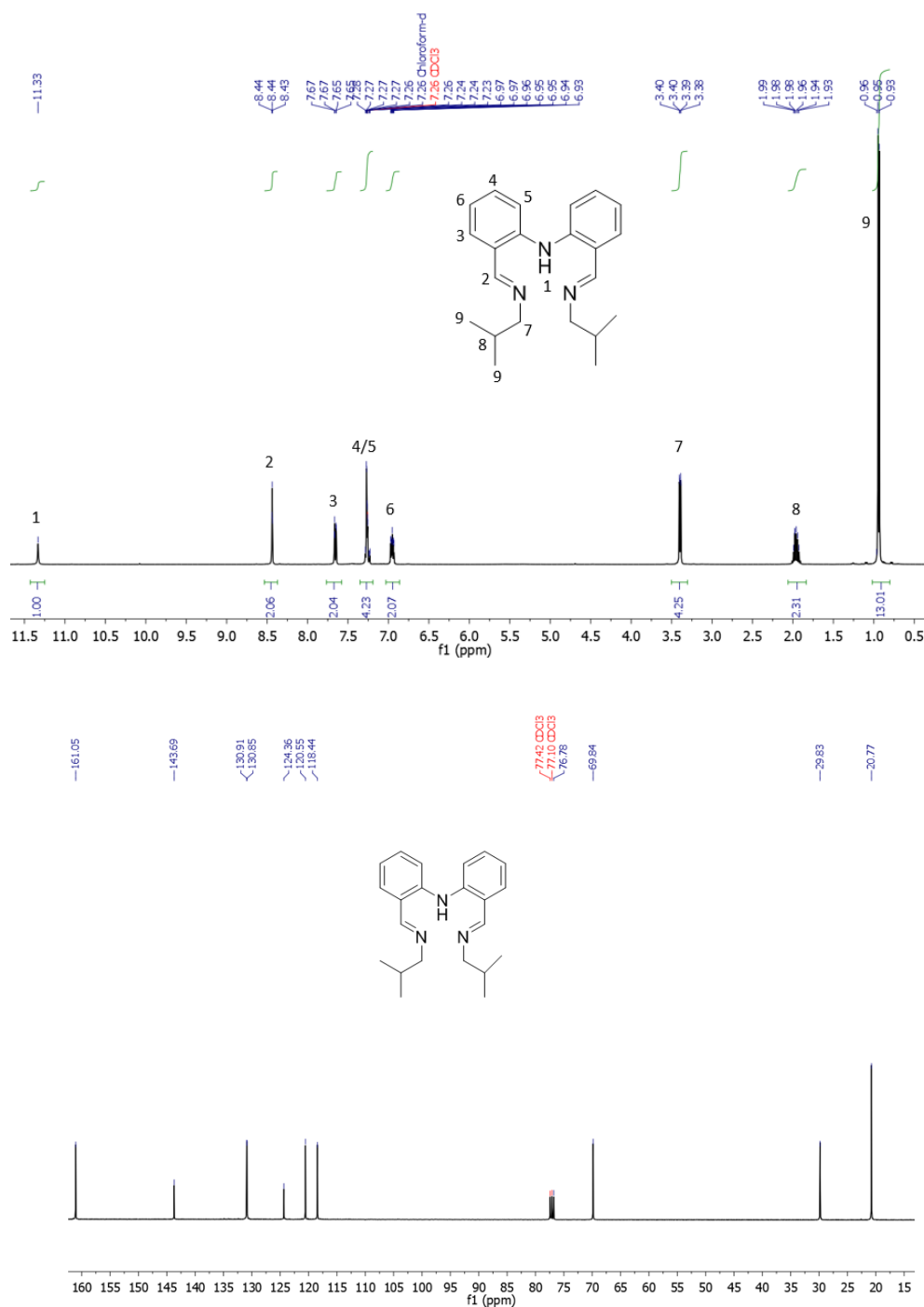


Figure S1: ¹H (upper spectrum) and ¹³C (lower spectrum) NMR of HL^{Open} in CDCl₃ (298 K)

Complex synthesis:

[Zn₂(L^{Et})(HMDS)₂] (**1**) and [Zn₂(L^{Pr})(HMDS)₂] (**2**): Under a nitrogen atmosphere, H₂L^{Et} or H₂L^{Pr} (200 mg, 1 eq.) was suspended in THF (5 mL). Zn(HMDS)₂ was dissolved in THF (2 mL) and was added dropwise to the ligand slurry at 22 °C. Upon the addition, the solution colour changed from yellow to deep red. The solution was stirred for 24 h at 25 °C and 2 h at 50 °C to push the

reaction to completion. The THF was removed and the crude product was dried under reduced pressure. **1** and **2** were isolated as red powders after several washing with cold hexane. (Yield: **1**: 86 %, 350 mg, **2**: 78 %, 240 mg).

1: ^1H NMR (400 MHz, d_8 -THF, 198 K) δ 8.71 (s, 2H, HC=N), 7.69 (s, 2H, HC=N), 7.60 (d, J = 7.6 Hz, 2H, *m*-Ph), 7.49 (d, J = 8.2 Hz, 2H, *o*-Ph), 7.39 (t, J = 7.5 Hz, 2H, *p*-Ph), 7.10 (d, J = 8.8 Hz, 2H, *o*-Ph), 7.02 (t, J = 7.5 Hz, 2H, *p*-Ph), 6.86 (t, J = 7.8 Hz, 2H, *p*-Ph), 6.25 (d, J = 7.5 Hz, 2H, *m*-Ph), 5.92 (t, J = 7.3 Hz, 2H, *p*-Ph), 4.47 (d, J = 11.5 Hz, 2H, N-CHH-CH₂), 4.30 (t, J = 11.6 Hz, 2H, N-CHH-CH₂), 4.17 (d, J = 11.7 Hz, 2H, N-CHH-CH₂), 3.41 (t, J = 11.6 Hz, 2H, N-CHH-CH₂), -0.11 (s, 16H, Si(CH₃)₂), -0.37 (s, 17H, Si(CH₃)₂). ^{13}C NMR (101 MHz, THF, 198 K) δ 173.8 (HC=N), 171.9 (HC=N), 152.7 (*i*-Ph), 152.6 (*i*-Ph), 139.2 (*m*-Ph), 135.3 (*m*-Ph), 133.7 (*m*-Ph), 132.6 (*m*-Ph), 128.0 (*o*-Ph), 124.8 (*o*-Ph), 121.2 (*p*-Ph), 117.8 (*o*-Ph), 115.7 (*p*-Ph), 113.2 (*o*-Ph), 65.8 (N-CH₂-CH₂), 60.2 (N-CH₂-CH₂), 6.4 (Si(CH₃)₂), 5.5 (Si(CH₃)₂). Elemental analysis for C₄₄H₆₄N₈Si₄Zn₂. (948 g/mol): Calculated: C, 55.74; H, 6.80; N 11.82 %. Found: C, 55.56; H, 6.76; N, 11.67 %.

2: ^1H NMR (400 MHz, d_8 -THF, 298 K) δ 8.30 (s, 2H, HC=N), 8.26 (s, 2H, HC=N), 7.27 (d, J = 8.5 Hz, 4H,), 7.24 – 7.18 (m, 2H), 7.12 (td, J = 8.6, 4.2 Hz, 5H), 6.74 – 6.50 (m, 5H), 4.30 (dt, J = 12.0, 6.5 Hz, 2H), 4.16 (td, J = 11.7, 3.7 Hz, 2H), 3.65 – 3.53 (m, 3H), 3.44 (dt, J = 11.6, 7.9 Hz, 2H), 2.39 (dddd, J = 15.7, 11.5, 7.9, 4.2 Hz, 1H), 2.07 (tq, J = 18.2, 6.3 Hz, 1H), 1.92 (s, 2H), -0.15 (s, 19H), -0.26 (s, 17H). ^{13}C NMR (101 MHz, d_8 -THF) δ 170.50 (HC=N), 170.17 (HC=N), 152.48 (*i*-Ph), 135.51 (*m*-Ph), 132.32 (*p*-Ph), 121.59 (*o*-Ph), 119.13 (*m*-Ph), 58.32 (N-CH₂-CH₂), 57.81 (N-CH₂-CH₂), 33.94 (CH₂-CH₂-CH₂), 5.27 (Si-(CH₃)₂), 4.90 (Si-(CH₃)₂). C₄₆H₆₈N₈Si₄Zn₂ (948 g/mol): Calculated: C, 56.60; H, 7.02; N 11.48 %. Found: C, 56.42; H, 6.83; N, 11.27 %.

3 was synthesized from the reaction of **HL**^{open} (100 mg, 0.3 mmol, 1 eq.) with Zn(HMDS)₂ (115 mg, 0.3 mg, 1 eq.) in 5 mL of THF. The crude product was washed with hexane, filtrated and dried under reduced pressure (Yield: 55 %, 91 mg). More products was obtained by crystallisation of the filtrate at -40 °C overnight (Total yield: 72 %, 120 mg).

^1H NMR (400 MHz, C₆D₆) δ 7.59 (s, 2H, CH=N), 7.39 (d, J = 8.8 Hz, 2H, *m*-Ph), 7.00 (m, 4H, *p*-Ph + *o*-Ph), 6.58 (t, J = 7.5, 2H, *m*-Ph), 3.54 (br. s, 2H, N-CH₂-C), 2.97 (br. s, 2H, N-CH₂-C), 2.06 (sep, J = 6.7 Hz, 2H), 0.72 (br. s, 12H), 0.20 (s, 18H, N(Si(CH₃)₃)₂). ^{13}C NMR (101 MHz, C₆D₆) δ 168.50 (CH=N), 152.66 (*o*-Ph), 135.58 (*o*-Ph), 132.51 (*p*-Ph), 117.01 (*m*-Ph), 69.13 (N-CH₂-C), 29.06 (CH₂-CH-(CH₃)₂), 19.70 ((CH₃)₂), 5.64 (N(Si(CH₃)₃)₂).

Typical Polymerization procedure: In a glove box, rac-LA was dissolved in THF and was injected to an initiator (5 mg) solution in THF (0.2 mL) at 25 °C. The concentration of rac-LA was kept at 1 mol/L for all the polymerization reaction. For immortal polymerization studies, the required amount of isopropanol from a stock solution of isopropanol in THF [0.05 M] was added

on the rac-LA solution. For polymerization studies with alkoxide complexes, the alkoxide was generated *in-situ* by addition of two equivalents of isopropanol to the catalyst precursor. The solution was stirred for 30 min at 25 °C prior the addition of rac-LA. The rac-LA solution was added on to the initiator solution and the polymerization reaction was stirred at 25 °C. The reaction was followed by aliquoting and quenching the reaction mixture in hexane at different times. Aliquotes were analysed by ¹H NMR, homonuclear-decoupled ¹H NMR in CDCl₃ and by SEC in THF.

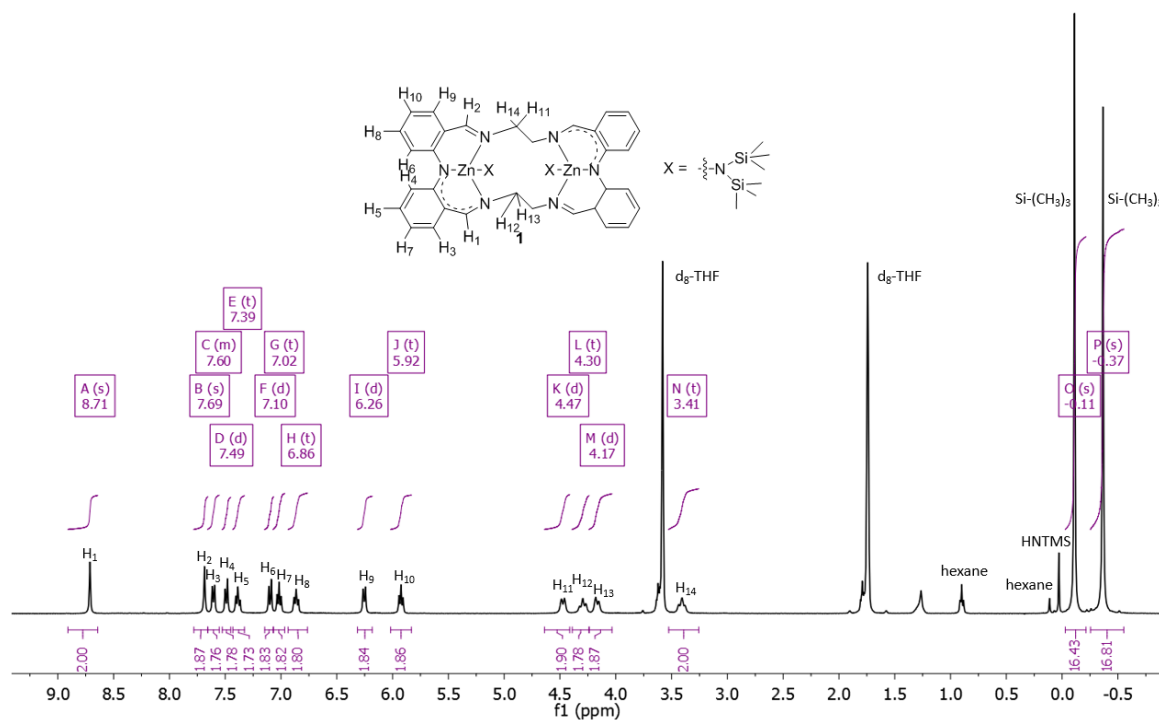


Figure S2: ¹H NMR of **1** (d₈-THF, 193 K)

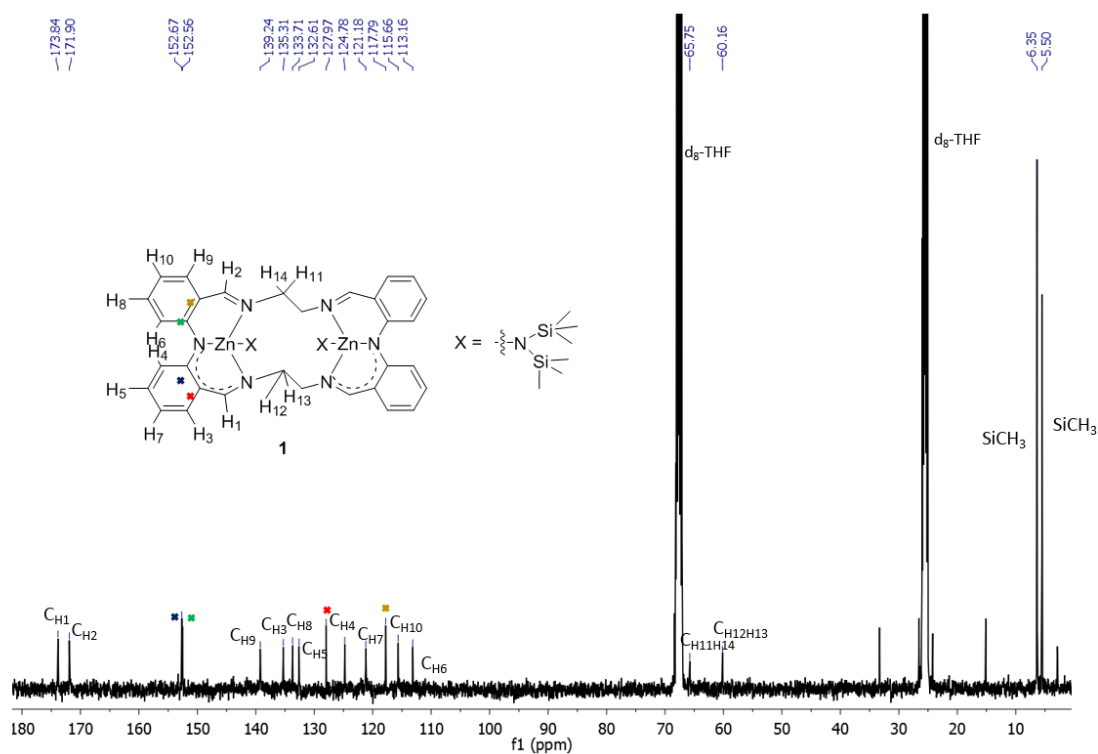


Figure S3: ^{13}C NMR of **1** (d_8 -THF, 193 K)

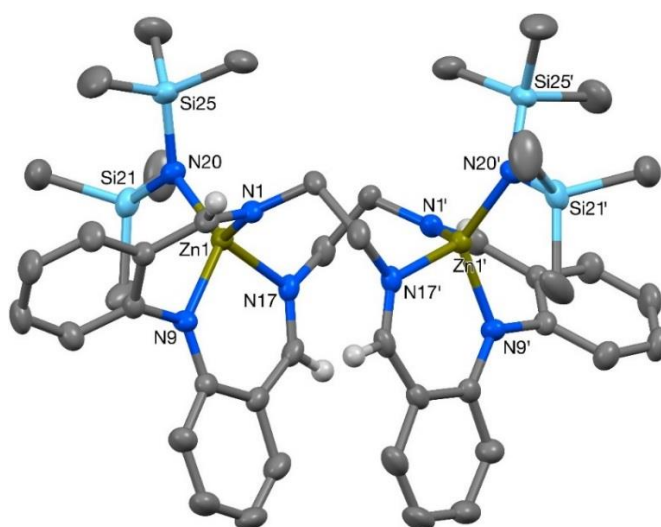


Figure S4: Molecular structure of **1**, presenting a C_2 symmetry with thermal ellipsoids at the 50% probability level, hydrogen atoms (apart from imine protons) and one THF molecule are omitted for clarity.

Crystal data for **1**: $\text{C}_{44}\text{H}_{64}\text{N}_8\text{Si}_4\text{Zn}_2 \cdot 2(\text{C}_4\text{H}_8\text{O})$, $M = 1092.34$, orthorhombic, $Pccn$ (no. 56), $a = 15.3644(5)$, $b = 15.7314(5)$, $c = 23.9599(10)$ Å, $V = 5791.2(4)$ Å³, $Z = 4$ (C_2 symmetry), $\rho_{\text{calcd}} = 1.253$ g cm⁻³, $\mu(\text{MoK}\alpha) = 0.955$ mm⁻¹, $T = 173$ K, red blocks, Agilent Xcalibur 3 E diffractometer; 5747 independent measured reflections ($R_{\text{int}} = 0.0286$), F^2 refinement,⁷ $R_1(\text{obs}) = 0.0422$, $wR_2(\text{all}) = 0.1115$, 4350 independent observed absorption-corrected reflections [$|F_o| > 4\sigma(|F_o|)$], $2\theta_{\text{max}} = 57^\circ$), 313 parameters. CCDC 1469823. The structure of **1** sits across a C_2 axis that bisects the $\text{N}(1)\cdots\text{N}(1A)$ and $\text{N}(17)\cdots\text{N}(17A)$ vectors.

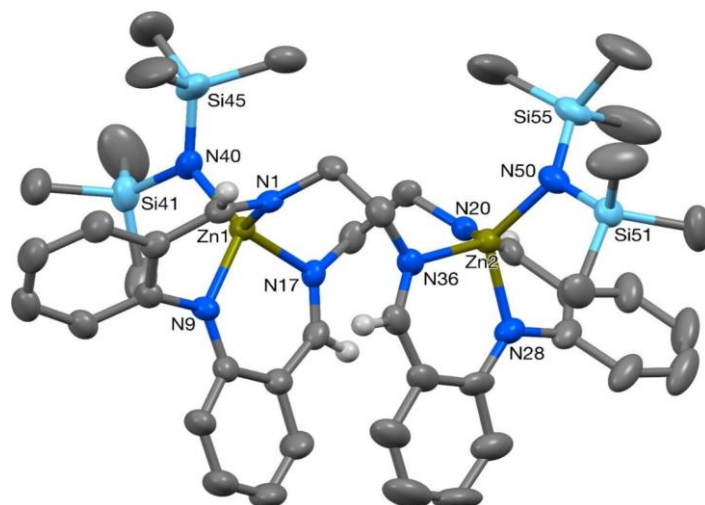


Figure S5: Molecular structure of **1b**, with thermal ellipsoids at the 50% probability level, hydrogen atoms (apart from imine protons) and a molecule of hexane are omitted for clarity.

Crystal data for 1b: $C_{44}H_{64}N_8Si_4Zn_2 \cdot 0.5(C_6H_{14})$, $M = 991.21$, monoclinic, $P2_1/n$ (no. 14), $a = 12.6935(3)$, $b = 15.0811(3)$, $c = 28.2654(6)$ Å, $\beta = 100.446(2)^\circ$, $V = 5321.2(2)$ Å³, $Z = 4$, $\rho_{\text{calcd}} = 1.237$ g cm⁻³, $\mu(\text{MoK}\alpha) = 1.030$ mm⁻¹, $T = 173$ K, orange blocks, Agilent Xcalibur 3 E diffractometer; 10597 independent measured reflections ($R_{\text{int}} = 0.0285$), F^2 refinement,⁷ $R_1(\text{obs}) = 0.0451$, $wR_2(\text{all}) = 0.1087$, 8338 independent observed absorption-corrected reflections [$|F_o| > 4\sigma(|F_o|)$], $2\theta_{\text{max}} = 56^\circ$], 577 parameters. CCDC 1469824. The Si51-based SiMe3 group in the structure of **1b** was found to be disordered. Two orientations were identified of *ca.* 78 and 22% occupancy, their geometries were optimised, the thermal parameters of adjacent atoms were restrained to be similar, and only the non-hydrogen atoms of the major occupancy orientation were refined anisotropically (those of the minor occupancy orientation were refined isotropically).

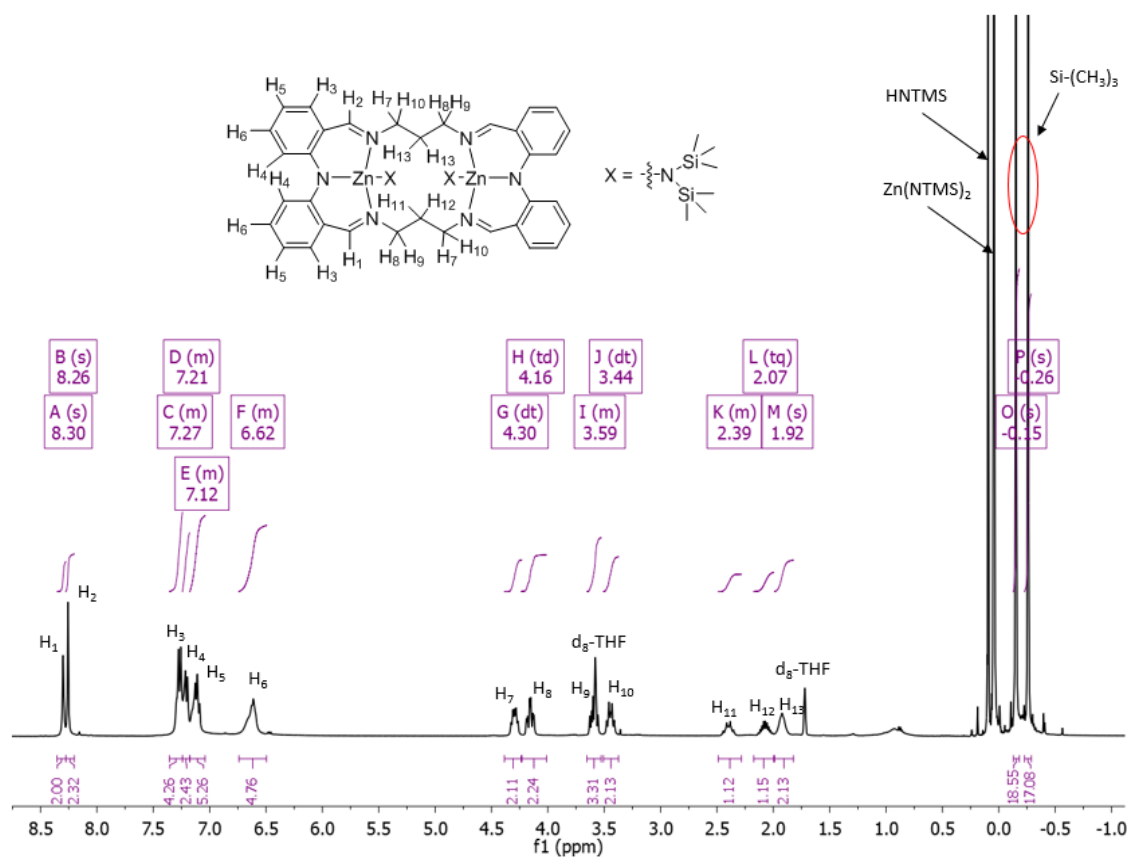


Figure S6: ¹H NMR of 2 (d₈-THF, 298 K)

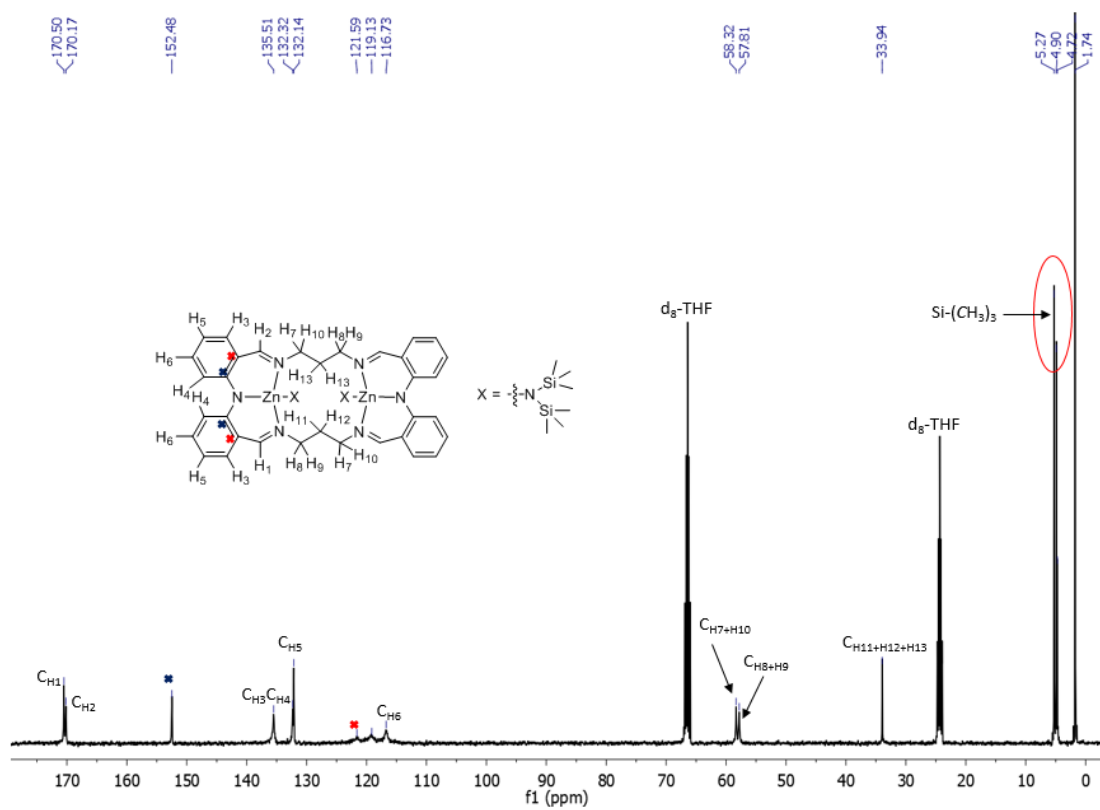


Figure S7: ¹³C NMR of 2 (d₈-THF, 298 K)

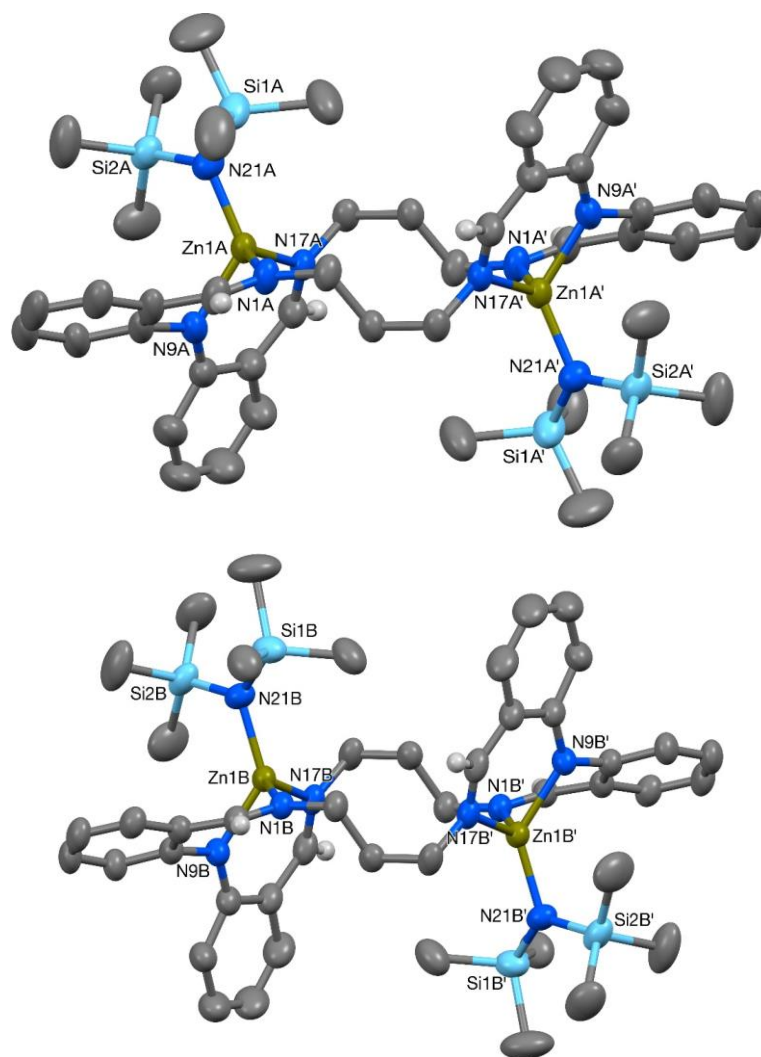


Figure S8: Molecular structure of **2** containing two independent molecules with thermal ellipsoids at the 50% probability level, hydrogen atoms (apart from imine protons) and one molecule of hexane are omitted for clarity.

Crystal data for **2**: $C_{46}H_{68}N_8Si_4Zn_2 \cdot C_6H_{14}$, $M = 1062.35$, monoclinic, $P2_1/c$ (no. 14), $a = 21.5374(2)$, $b = 20.73239(18)$, $c = 13.04210(15)$ Å, $\beta = 96.7198(10)^\circ$, $V = 5783.59(10)$ Å³, $Z = 4$ (2 independent C_2 -symmetric molecules), $\rho_{\text{calcd}} = 1.220$ g cm⁻³, $\mu(\text{Cu}_{K\alpha}) = 2.114$ mm⁻¹, $T = 173$ K, dark orange blocks, Agilent Xcalibur PX Ultra A diffractometer; 11174 independent measured reflections ($R_{\text{int}} = 0.0190$), F^2 refinement,⁷ $R_1(\text{obs}) = 0.0536$, $wR_2(\text{all}) = 0.1654$, 9097 independent observed absorption-corrected reflections [$|F_o| > 4\sigma(|F_o|)$], $2\theta_{\text{max}} = 148^\circ$, 632 parameters. CCDC 1469825. The structure of **2** contains two independent molecules (**2-A** and **2-B**), both of which sit across centres of symmetry.

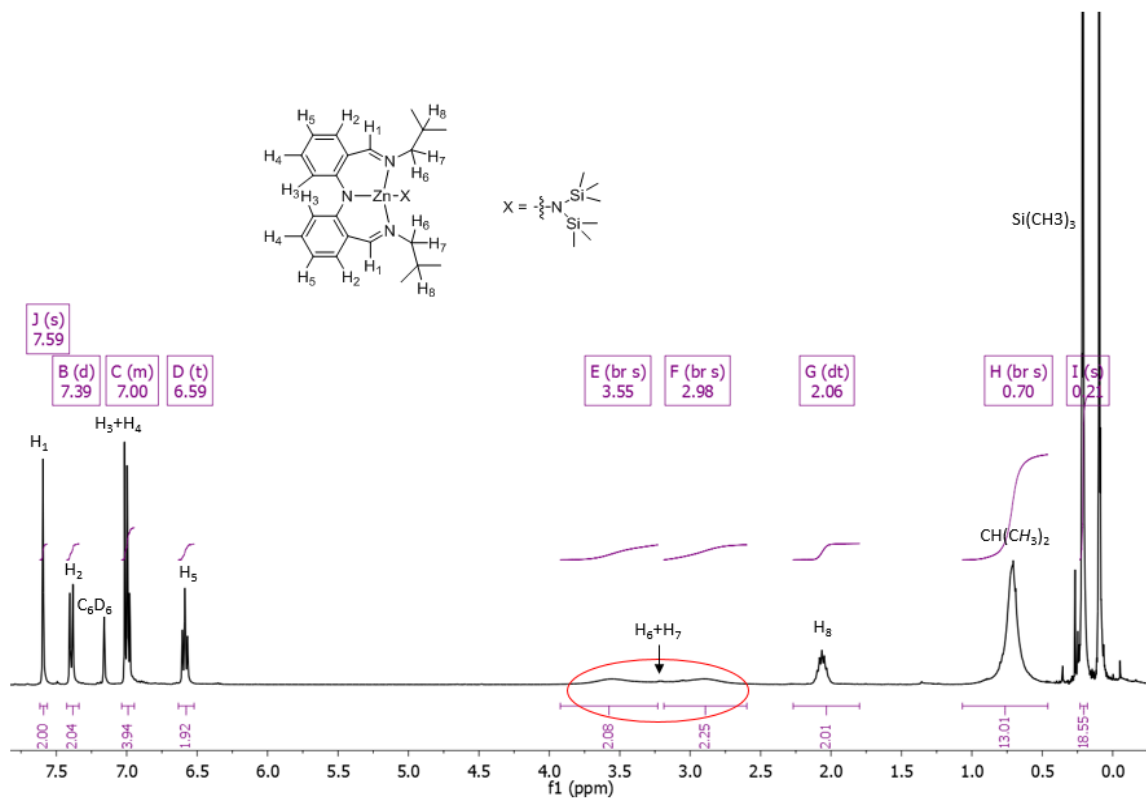


Figure S9: 1H NMR of **3** (C_6D_6 , 298 K)

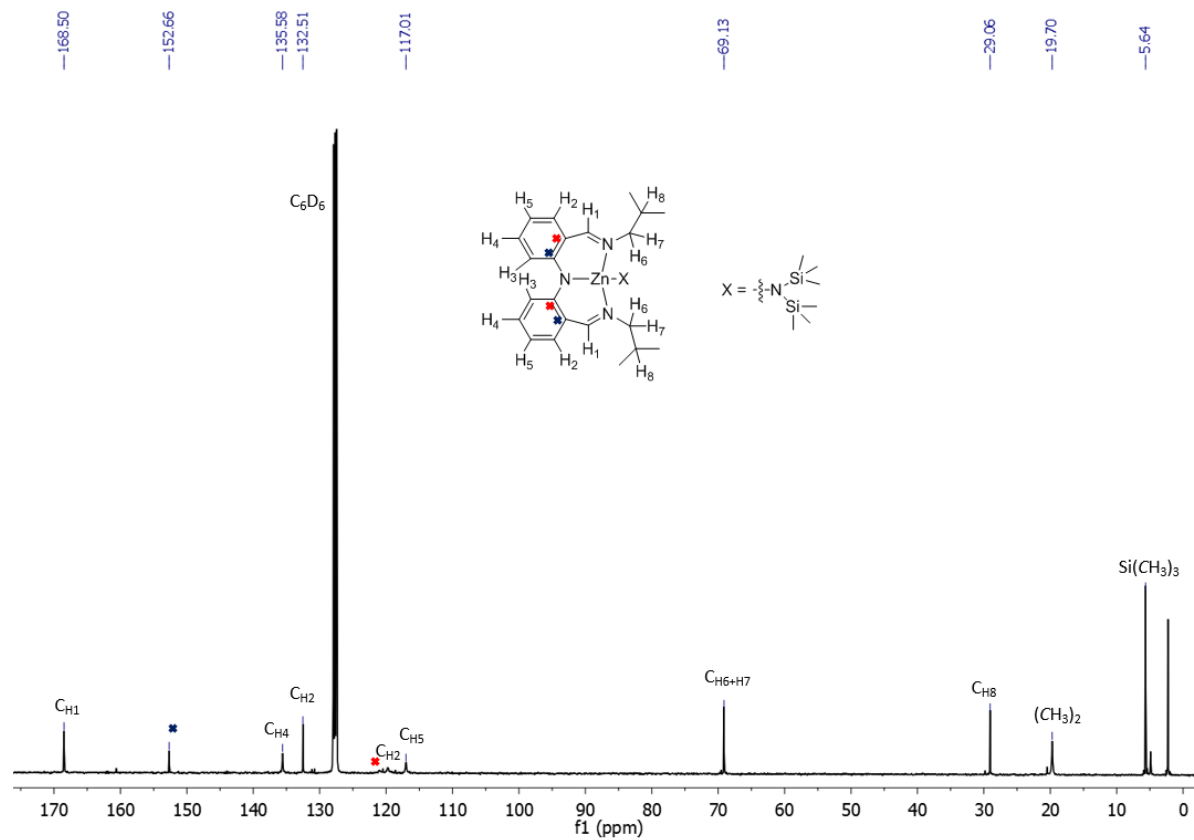


Figure S10: ^{13}C NMR of **3** (C_6D_6 , 298 K)

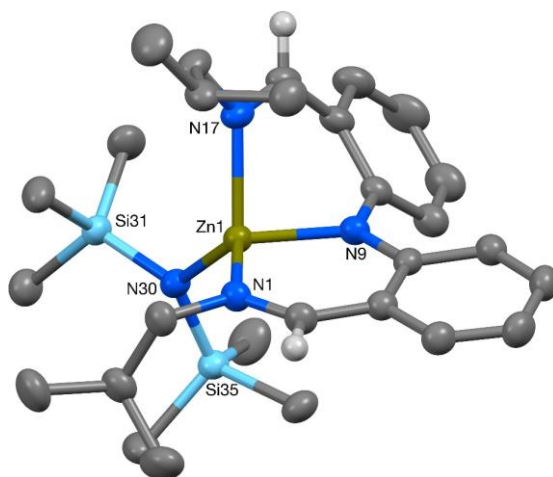


Figure S11: Molecular structure of **3**, with thermal ellipsoids at the 50% probability level, hydrogen atoms (apart from the imine protons) omitted for clarity.

Crystal data for **3**: $C_{28}H_{46}N_4Si_2Zn$, $M = 560.24$, monoclinic, $P2_1/n$ (no. 14), $a = 9.70000(12)$, $b = 13.84428(17)$, $c = 23.2122(3)$ Å, $\beta = 98.8744(13)^\circ$, $V = 3079.85(7)$ Å³, $Z = 4$, $\rho_{\text{calcd}} = 1.208$ g cm⁻³, $\mu(\text{Cu}_{K\alpha}) = 2.009$ mm⁻¹, $T = 173$ K, orange blocks, Agilent Xcalibur PX Ultra A diffractometer; 5921 independent measured reflections ($R_{\text{int}} = 0.0228$), F^2 refinement,⁷ $R_1(\text{obs}) = 0.0299$, $wR_2(\text{all}) = 0.0815$, 5090 independent observed absorption-corrected reflections [$|F_o| > 4\sigma(|F_o|)$], $2\theta_{\text{max}} = 148^\circ$], 327 parameters. CCDC 1469826.

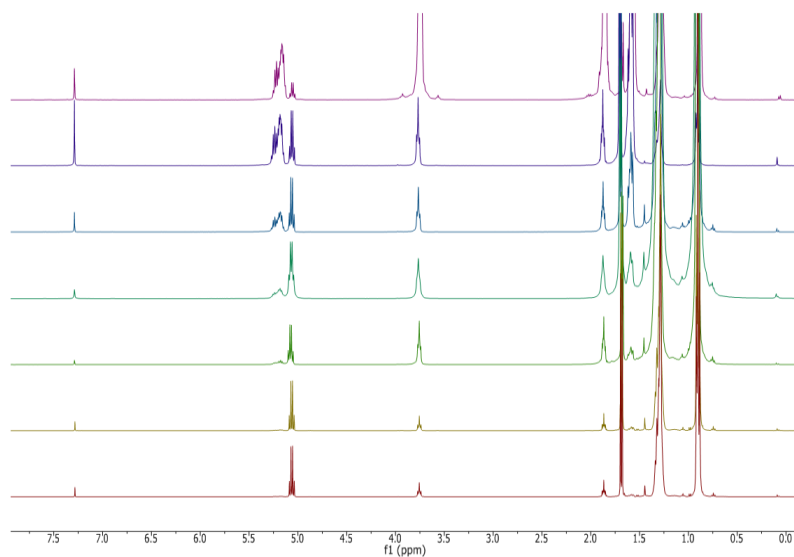


Figure S12: Stack of ¹H NMR spectra for the kinetic study of the polymerization of 1000 eq. of *rac*-LA using **1**. Conditions: [*rac*-LA] = 1M, THF, 25 °C.

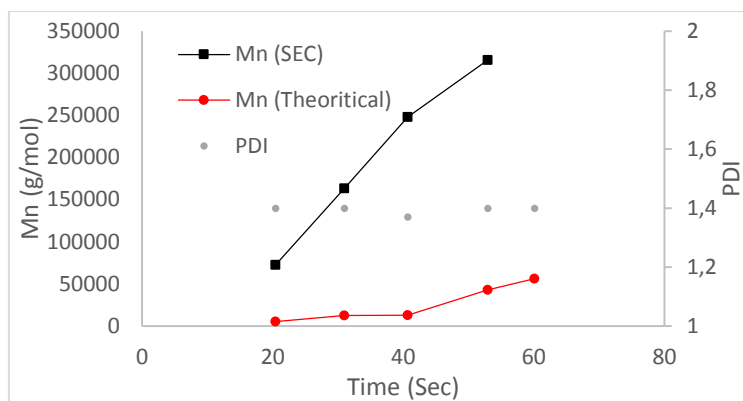


Figure S13: Plot of the molecular weight determined by SEC (■) and calculated (●) vs the conversion for **1** with 1000 equivalents of *rac*-LA. Conditions: [*rac*-LA] = 1M, THF, 25 °C

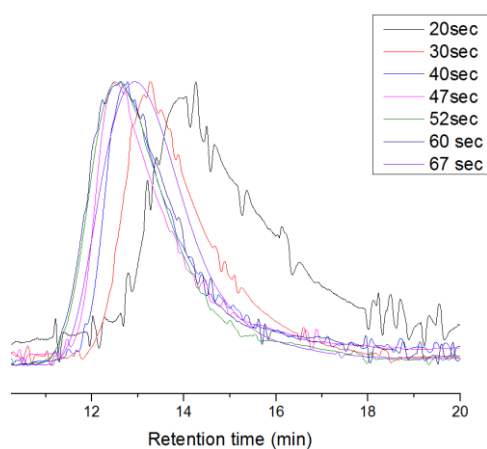


Figure S14: Overlap of SEC traces for **1** during the polymerization of 1000 equivalents of *rac*-LA. Conditions: [*rac*-LA] = 1M, THF, 25 °C

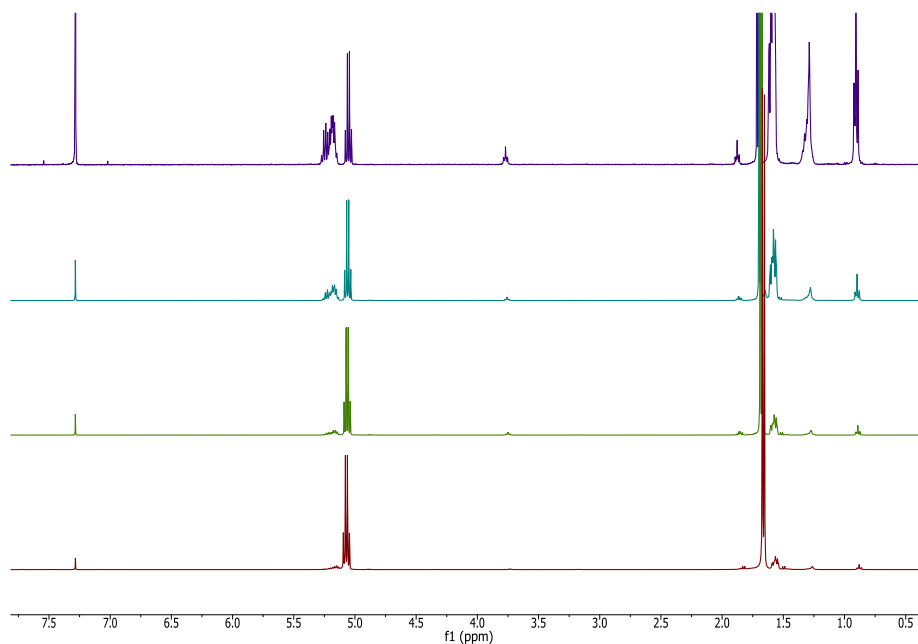


Figure S15 Stack of ¹H NMR spectra for the kinetic study of the polymerization of 1000 eq. of *rac*-LA using **2**. Conditions: [*rac*-LA] = 1M, THF, 25 °C.

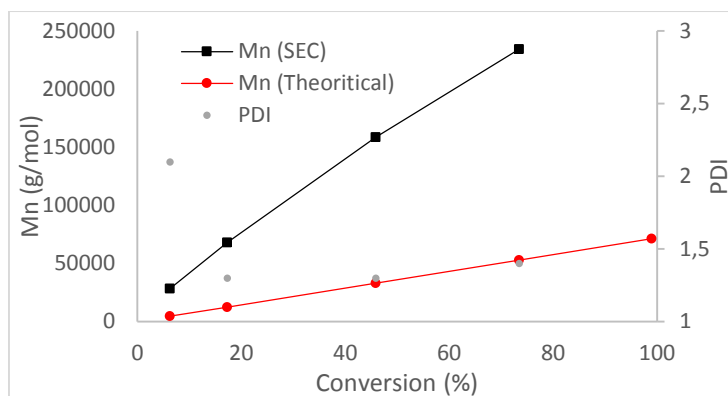


Figure S16: Plot of the molecular weight determined by SEC (■) and calculated (●) vs the conversion for **2** with 1000 equivalents of *rac*-LA. Conditions: [*rac*-LA] = 1M, THF, 25 °C

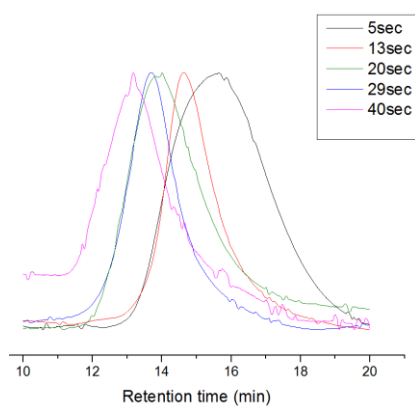


Figure S17: Overlap of SEC traces for **2** during the polymerization of 1000 equivalents of *rac*-LA. Conditions: [*rac*-LA] = 1M, THF, 25 °C

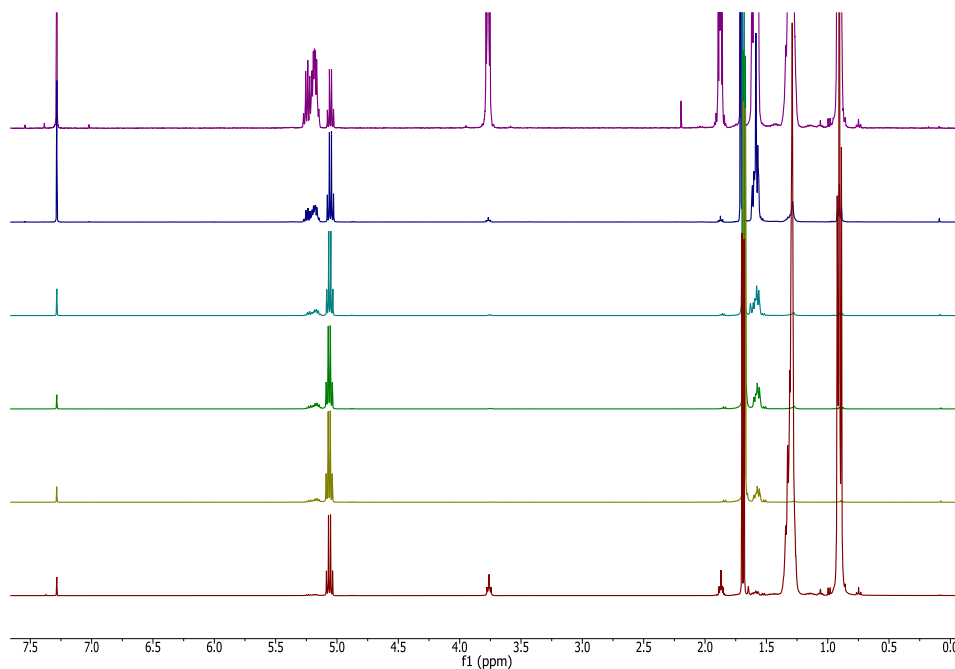


Figure S18: Stack of ^1H NMR spectra for the kinetic study of the polymerization of 1000 eq. of *rac*-LA using **3**. Conditions: [*rac*-LA] = 1M, THF, 25 °C.

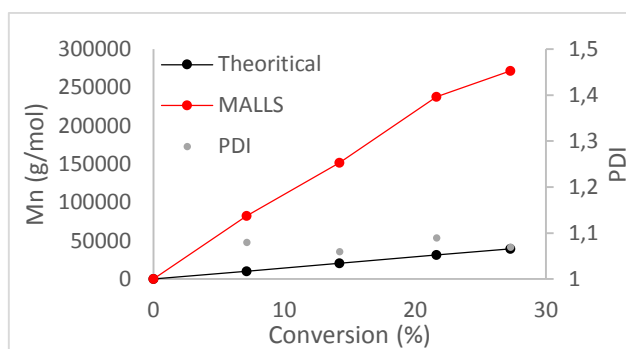


Figure S19: Plot of the molecular weight determined by SEC (■) and calculated (●) vs conversion for **3** with 1000 equivalents of *rac*-LA. Conditions: [*rac*-LA] = 1M, THF, 25 °C

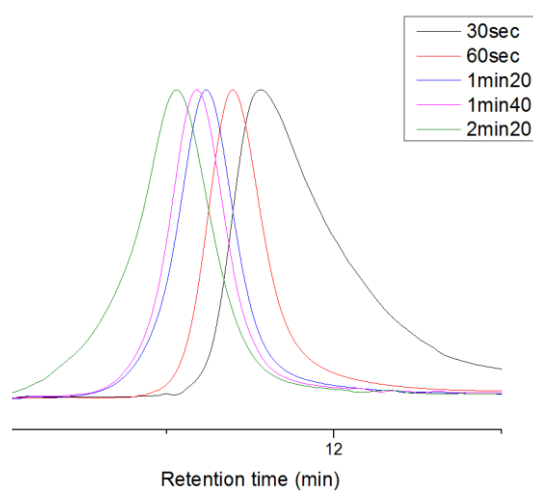


Figure S20: Overlap of SEC traces for **3** during the polymerization of 1000 equivalents of *rac*-LA. Conditions: [*rac*-LA] = 1M, THF, 25 °C

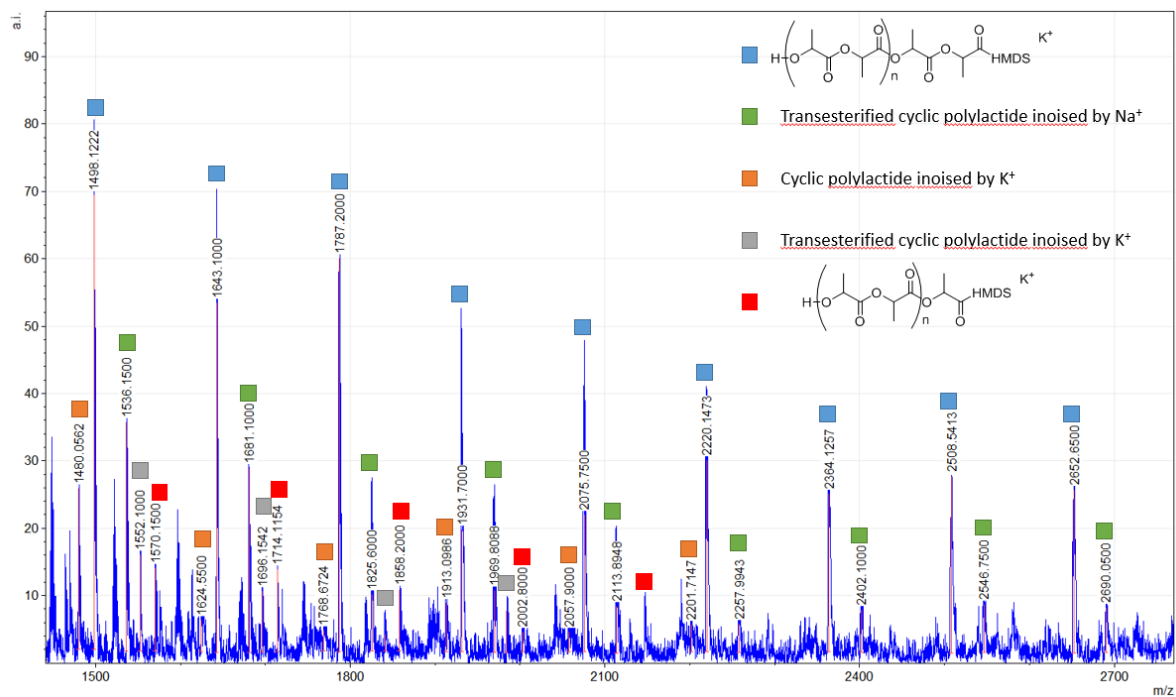


Figure S21: Typical example of MALDI-ToF spectrum obtained for monitoring a polymerization reaction with an amido catalyst. In this case, the polymer was synthesised using **2** at 25 °C in THF and 1000 eq. of rac-LA.

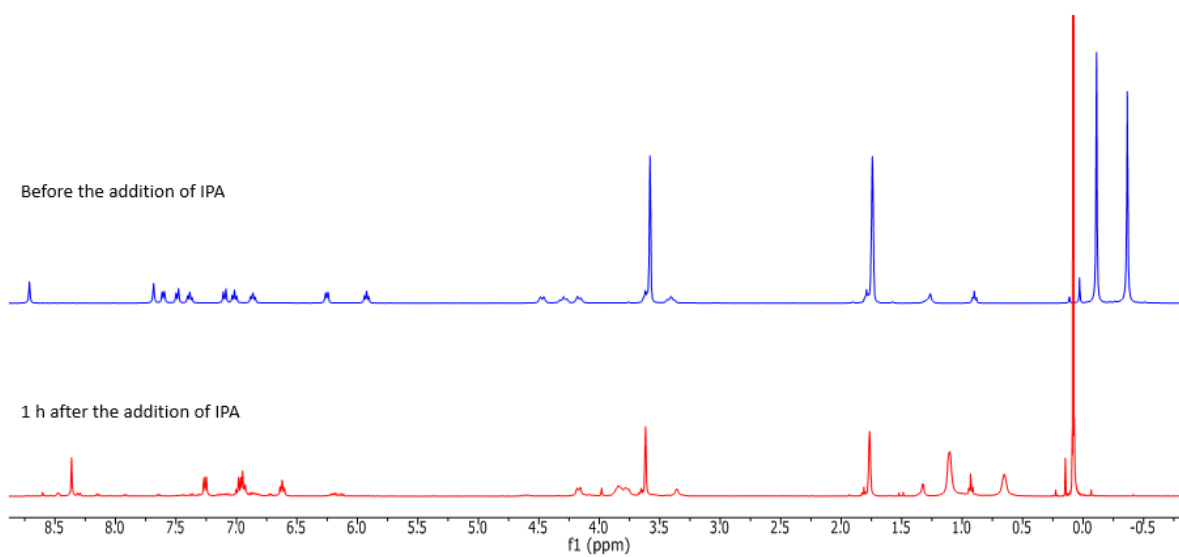


Figure S22: Overlaid of ¹H NMR of the reaction of **1** with 2 eq. of IPA (*d*₈-THF, 298 K), before the addition of IPA (upper spectrum), 1 h after the addition of IPA (lower spectrum).

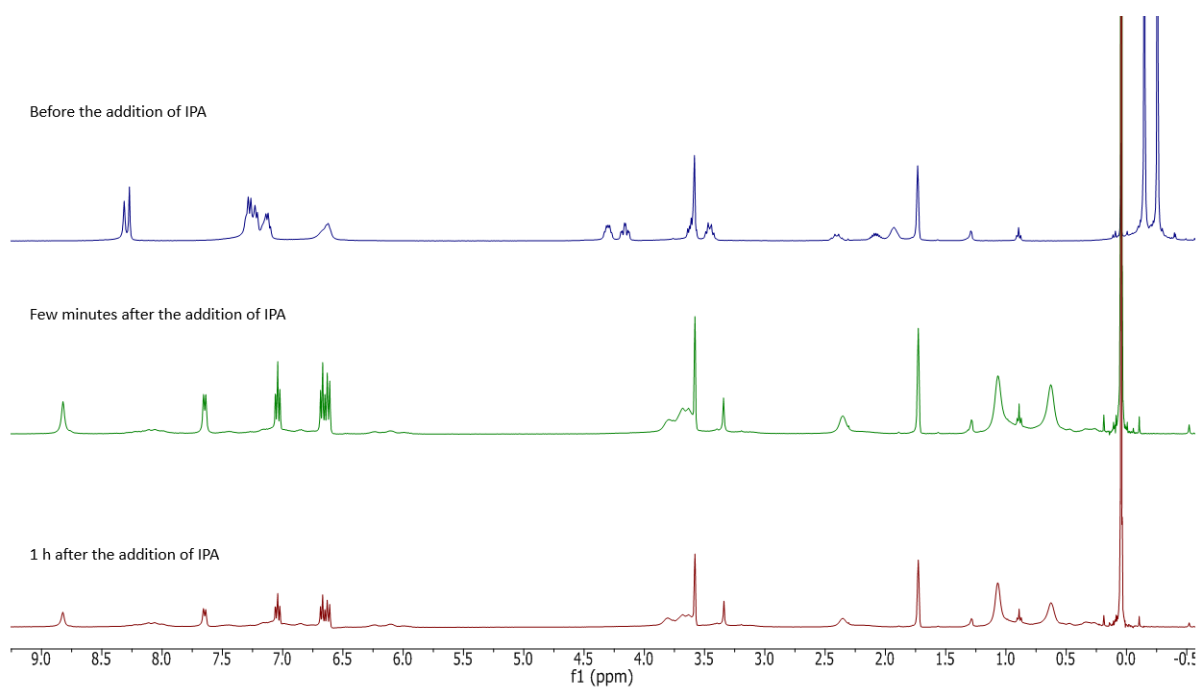


Figure S23: Overlaid of ^1H NMR of the reaction of **2** with 2 eq. of IPA (d_8 -THF, 298 K), before the addition of IPA (upper spectrum), few minutes after the addition of IPA (middle spectrum) and 1 h after the addition of IPA (lower spectrum).

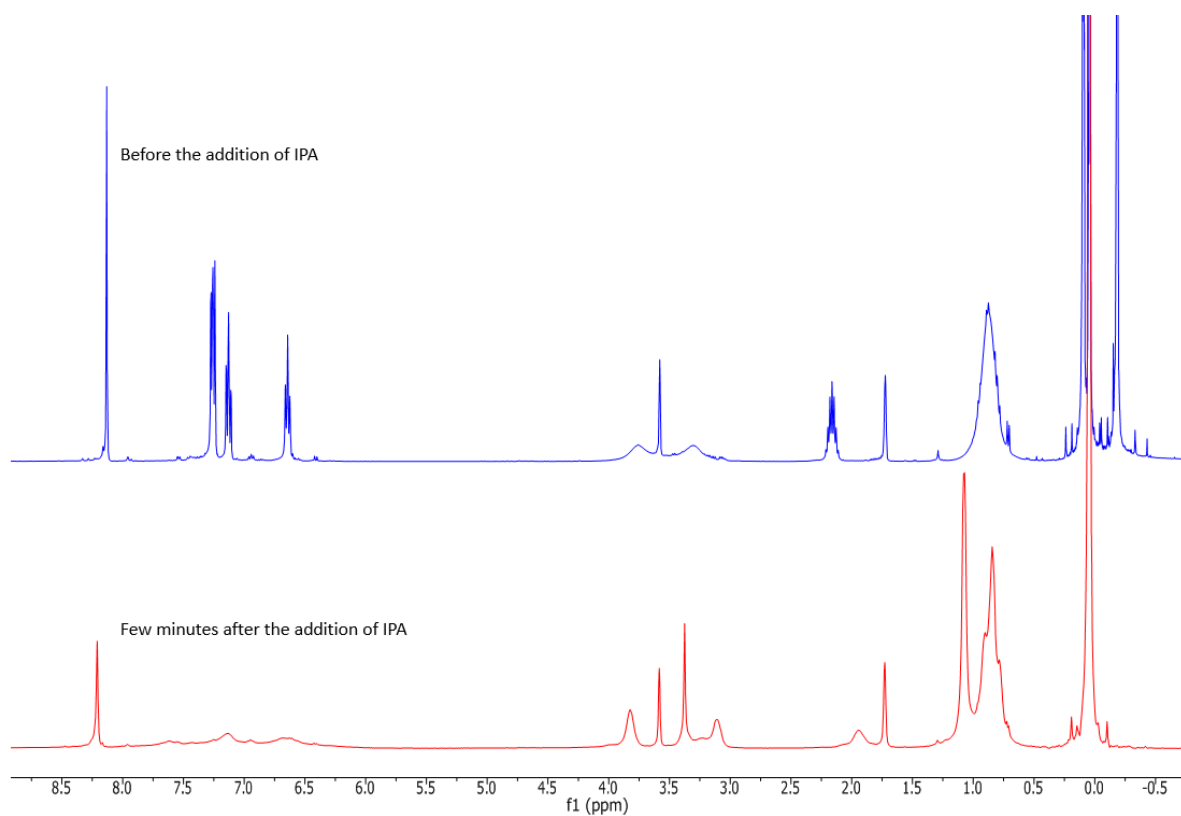


Figure S24: Overlaid of ^1H NMR of the reaction of **3** with 1 eq. of IPA (d_8 -THF, 298 K), before the addition of IPA (upper spectrum), few minutes after the addition of IPA (lower spectrum).

Table S1: rac-LA polymerization at different loading at 25 °C using 1, 2, 3, 4, 5 and 6.

Entry	Cat	IPA (eq)	Loading (mol%)	Time (s)	Conv. ^a (%)	Mn(exp) ^b Kg/mol	PDI ^b	Mn(cld) ^c Kg/mol	k _{obs} (s ⁻¹) ^d
1	4	0	0.1	8 x 3600	48	50	1.10	70	2.4 x 10 ⁻⁵
2	5	0	0.1	126	93	53	1.04	67	0.018
3	6	0	0.1	126	97	49	1.09	70	0.029
4	1	10	0.1	29	97	14	1.07	14	0.139
5	2	10	0.1	34	91	13	1.03	13	0.079
6	3	10	0.1	80	92	13	1.08	13	0.038
1	1	0	0.02	90	11	545	1.10	41	-
2	2	0	0.02	90	15	520	1.20	53	-
3	1	10	0.02	93	85	58	1.07	61	2.5 x 10 ⁻²
4	2	10	0.02	10 x 60	84	47	1.03	67	2.9 x 10 ⁻³
5	3	10	0.02	24 x 3600	0	-	-	-	-
6	1	20	0.01	5 x 60	70	46	1.05	47	-
7	2	20	0.01	3600	96	53	1.05	69	1.4 x 10 ⁻³
8	1	40	0.005	24 x 3600	10	-	-	-	-
9	2	40	0.005	3600	80	45	1.03	57	5 x 10 ⁻⁴
10	2	50	0.002	23 x 3600	50	52	1.02	78	-
11	A ^e	0	0.2	48 x 60	97	38	1.10	28	9 x 10 ⁻⁴
12	B ^f	0	0.1	13 x 60	99	100	1.40	142	1 x 10 ⁻³
13	C ^g	10	0.1	120	63	13	1.11	13	-
14	D ^h	0	0.009	8 x 3600	83	900	2.00	1344	-

Polymerization conditions: [rac-LA] = 1 M at 25 °C. ^aMonomer conversion determined by ¹H NMR spectroscopy (CDCl₃, 298 K). ^bExperimental molecular weight and PDI determined by SEC vs polystyrene standards and corrected by a factor of 0.58. ^cMolecular weight calculated using Mn(theor) = conversion × [rac-LA]₀ / [number of metal centre] × M_{LA}. ^dDetermined from the slope of the linear plot of ln([rac-LA]₀/[rac-LA]_t) vs time. [e] A = BDIZnOiPr, [rac-LA] = 0.4 M, T = 20 °C in CH₂Cl₂.⁸ [f] B = halvesalenZnEt, CH₂Cl₂.⁹ [g] C = bis(morpholinomethyl)phenoxyZnEt, 10 equiv. of IPA / mol of catalyst, T = 60 °C in toluene.¹⁰ [h] D = Tin octanoate, temperature:110 °C, neat.¹¹

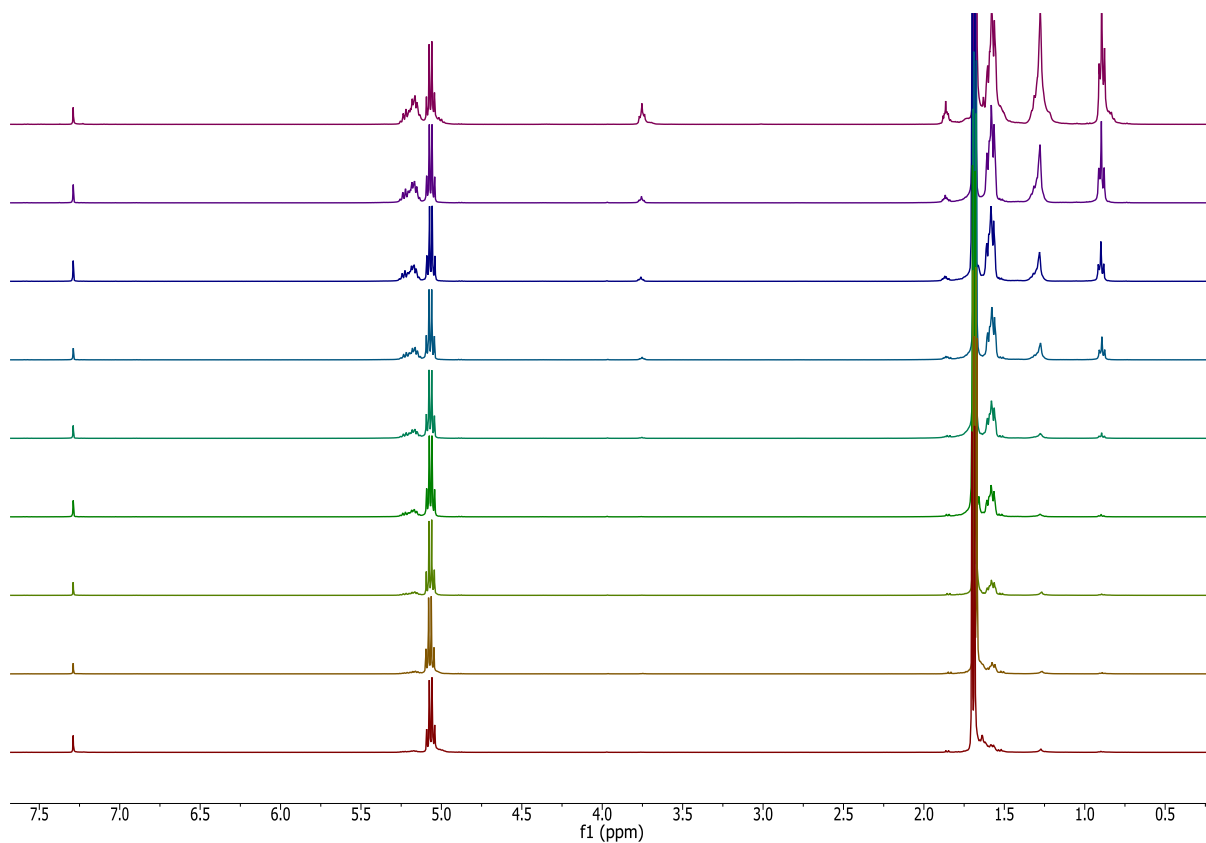


Figure S25: Stack of ^1H NMR spectra for the kinetic study of the polymerization of 1000 eq. of rac-LA using **4**. Conditions: $[\text{rac-LA}] = 1\text{M}$, THF, $25\text{ }^\circ\text{C}$.

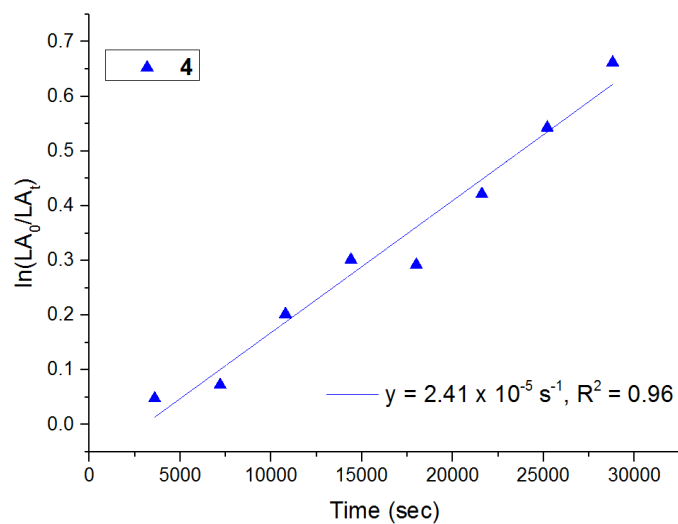


Figure S26: Plot of $\ln([\text{LA}]_0/[\text{LA}]_t)$ vs time for **4** (■) with 1000 equivalents of rac-LA. Conditions: $[\text{rac-LA}] = 1\text{M}$, THF, $25\text{ }^\circ\text{C}$

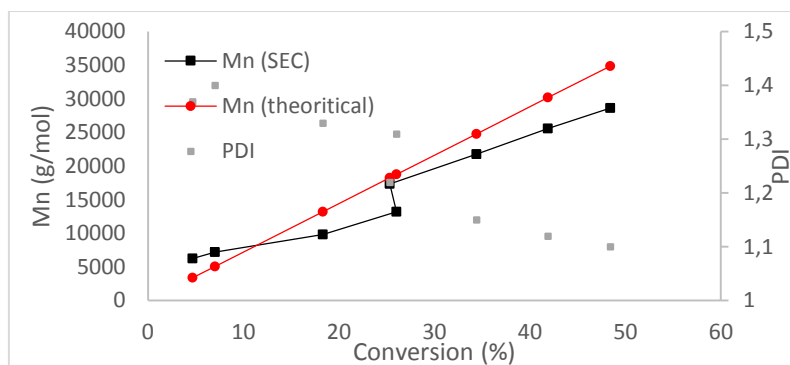


Figure S27: Plot of the molecular weight determined by SEC (■) and calculated (●) vs the conversion for **4** with 1000 equivalents of *rac*-LA. Conditions: [*rac*-LA] = 1M, THF, 25 °C

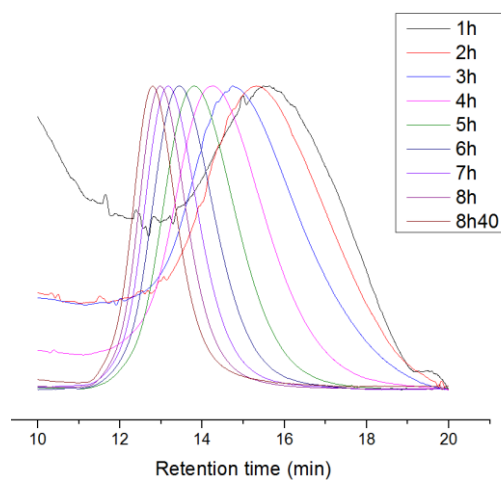


Figure S28: Overlap of SEC traces for **4** during the polymerization of 1000 equivalents of *rac*-LA. Conditions: [*rac*-LA] = 1M, THF, 25 °C

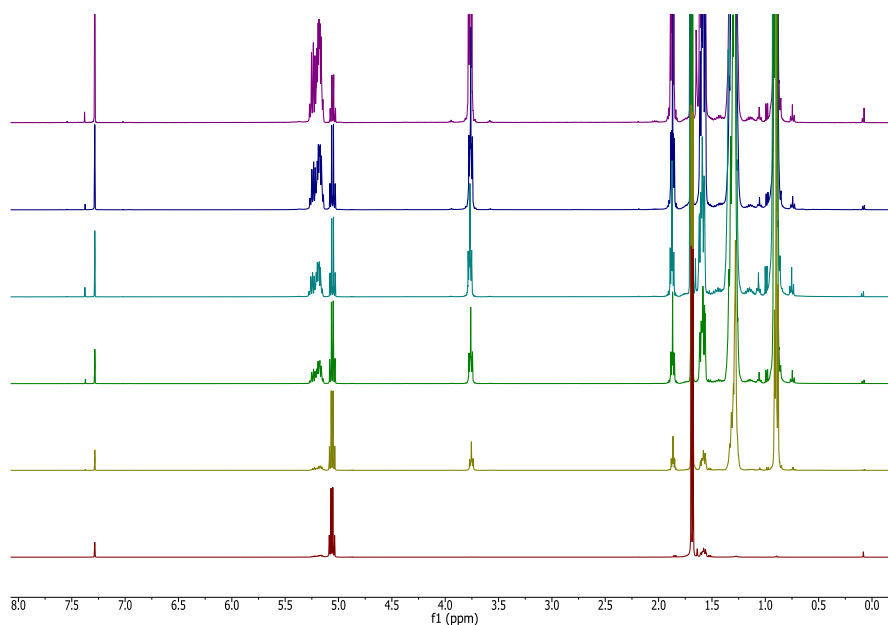


Figure S29: Stack of ^1H NMR spectra for the kinetic study of the polymerization of 1000 eq. of *rac*-LA using **5**. Conditions: [*rac*-LA] = 1M, THF, 25 °C.

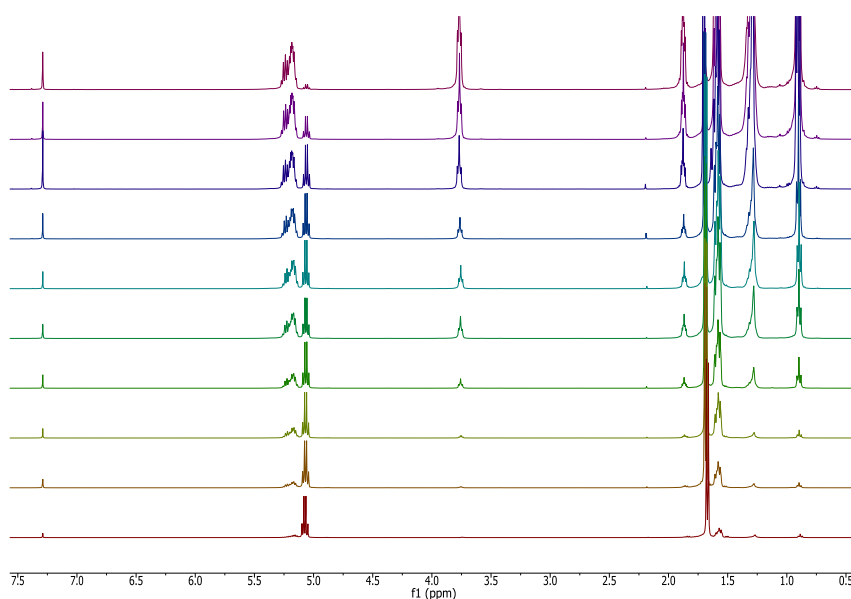


Figure S30: Stack of ^1H NMR spectra for the kinetic study of the polymerization of 1000 eq. of *rac*-LA using **6**. Conditions: $[\textit{rac}\text{-LA}] = 1\text{M}$, THF, 25°C .

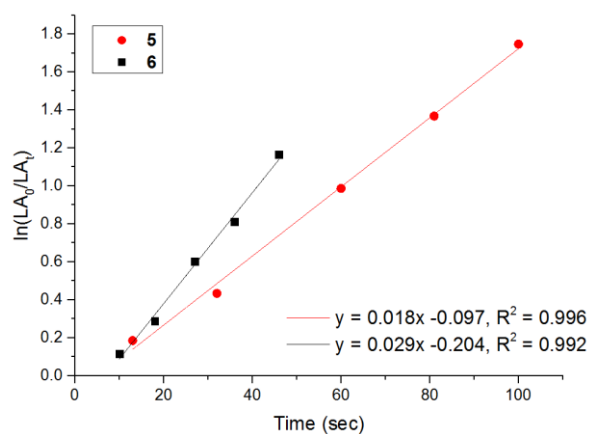


Figure S31: Plot of $\ln([LA_0]/[LA_i])$ vs time for **5** (●) and **6** (■) with 1000 equivalents of *rac*-LA. Conditions: $[\textit{rac}\text{-LA}] = 1\text{M}$, THF, 25°C

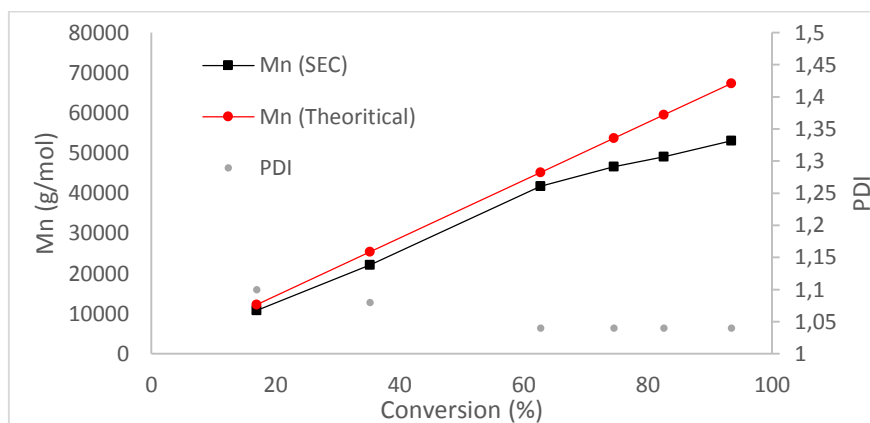


Figure S32: Plot of the molecular weight determined by SEC (■) and calculated (●) vs the conversion for **5** with 1000 equivalents of *rac*-LA. Conditions: $[\textit{rac}\text{-LA}] = 1\text{M}$, THF, 25°C

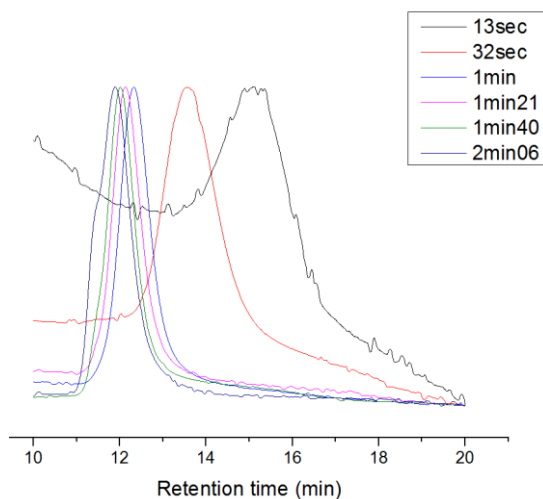


Figure S33: Overlap of SEC traces for **5** during the polymerization of 1000 equivalents of rac-LA. Conditions: [rac-LA] = 1M, THF, 25 °C

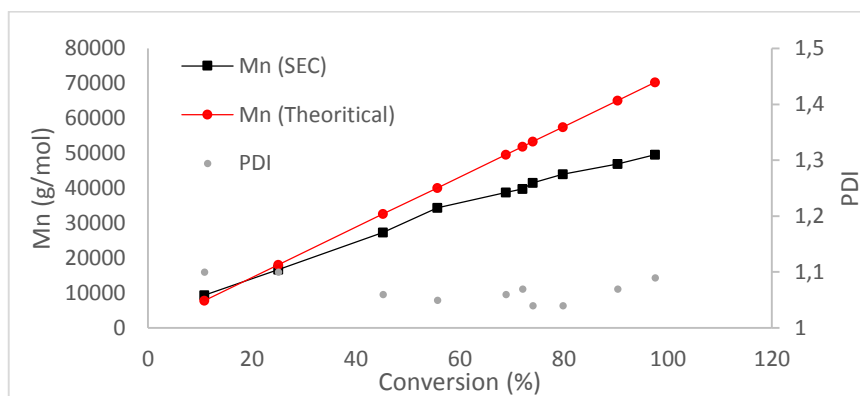


Figure S34: Plot of the molecular weight determined by SEC (■) and calculated (●) vs the conversion for **6** with 1000 equivalents of rac-LA. Conditions: [rac-LA] = 1M, THF, 25 °C

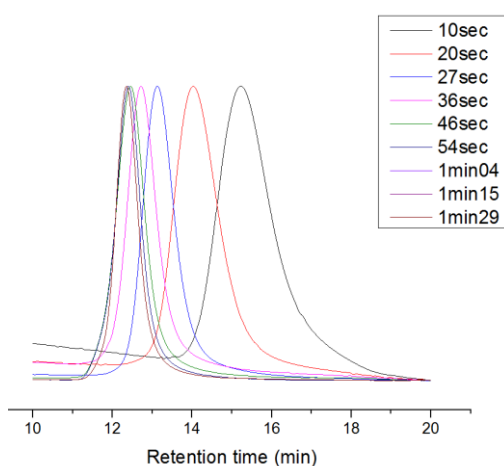


Figure S35: Overlap of SEC traces for **6** during the polymerization of 1000 equivalents of rac-LA. Conditions: [rac-LA] = 1M, THF, 25 °C

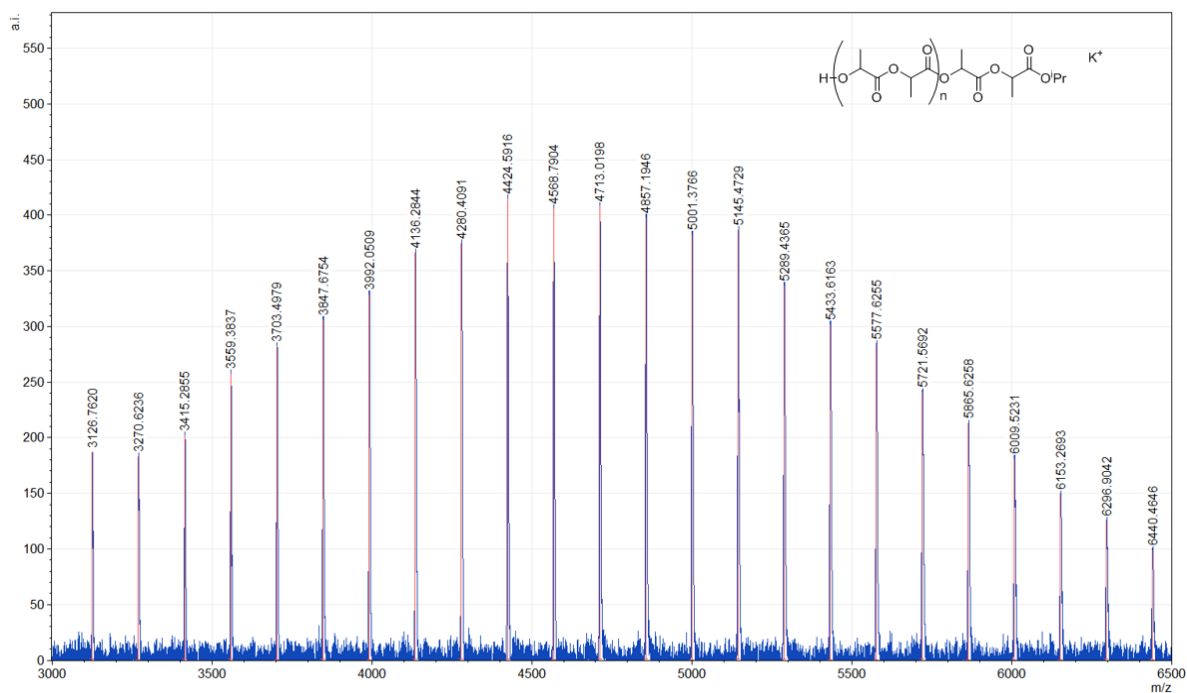


Figure S36: Typical example of MALDI-ToF spectrum obtained for a polymerization reaction using an alkoxide catalyst. In this case, the polymer was synthesised using **2** at 25 °C in THF and 1000 eq. of *rac*-LA.

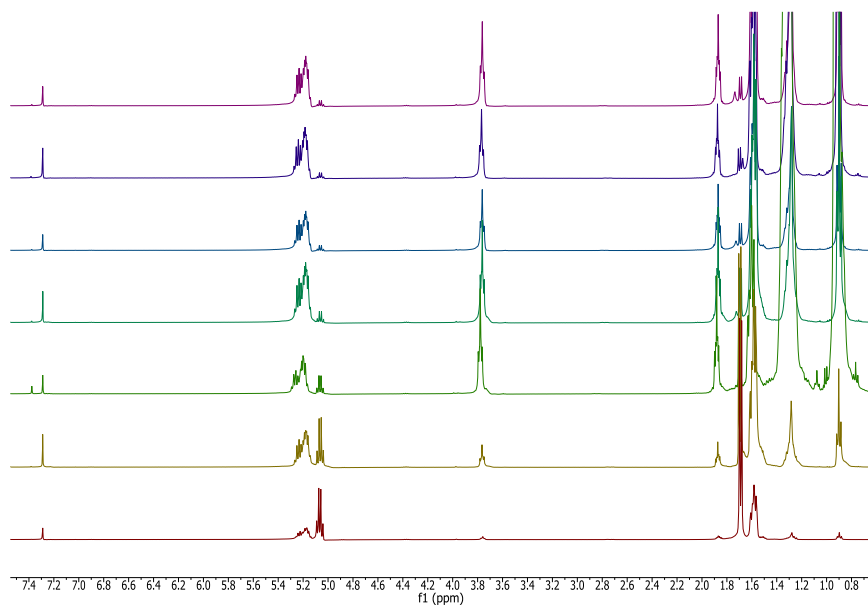


Figure S37: Stack of ^1H NMR spectra for the kinetic study of the polymerization of 1000 eq. of *rac*-LA using **1** in presence of 10 eq. of IPA. Conditions: $[\text{rac-LA}] = 1\text{M}$, THF, 25 °C

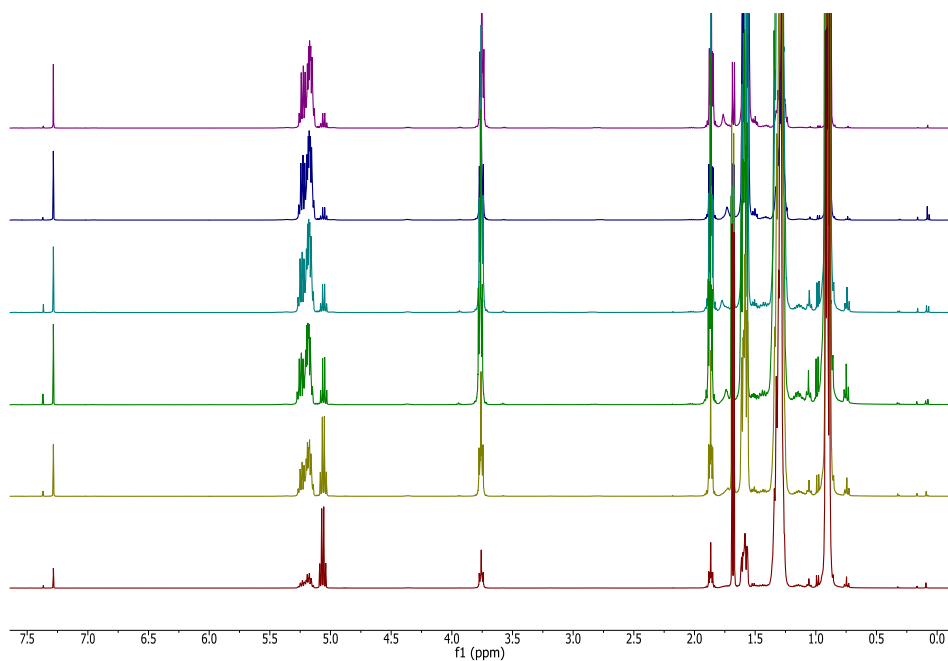


Figure S38: Stack of ^1H NMR spectra for the kinetic study of the polymerization of 1000 eq. of rac-LA using **2** in presence of 10 eq. of IPA. Conditions: $[\text{rac-LA}] = 1\text{M}$, THF, 25 °C

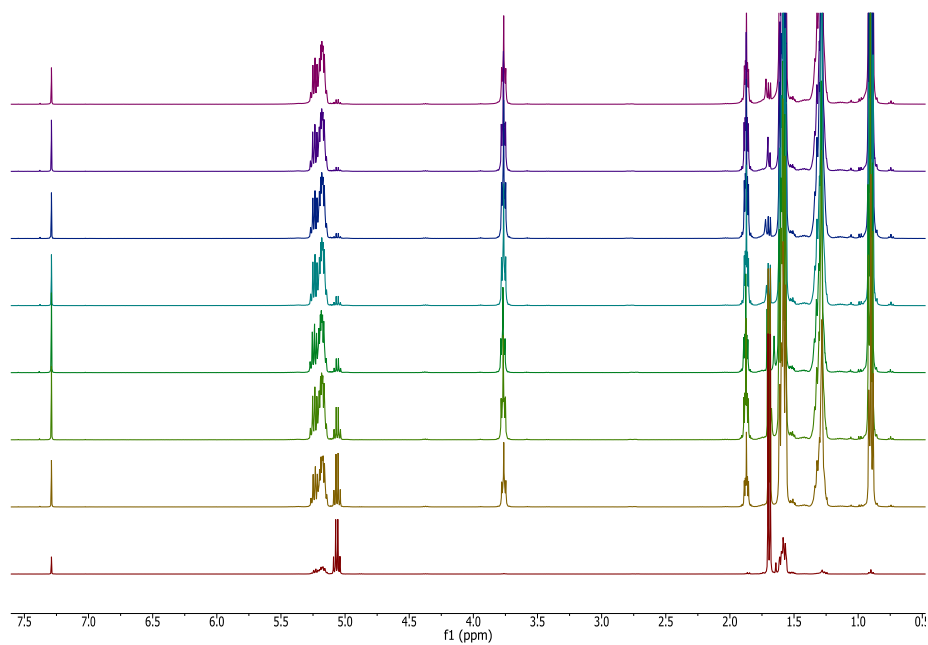


Figure S39: Stack of ^1H NMR spectra for the kinetic study of the polymerization of 1000 eq. of rac-LA using **3** in presence of 10 eq. of IPA. Conditions: $[\text{rac-LA}] = 1\text{M}$, THF, 25 °C

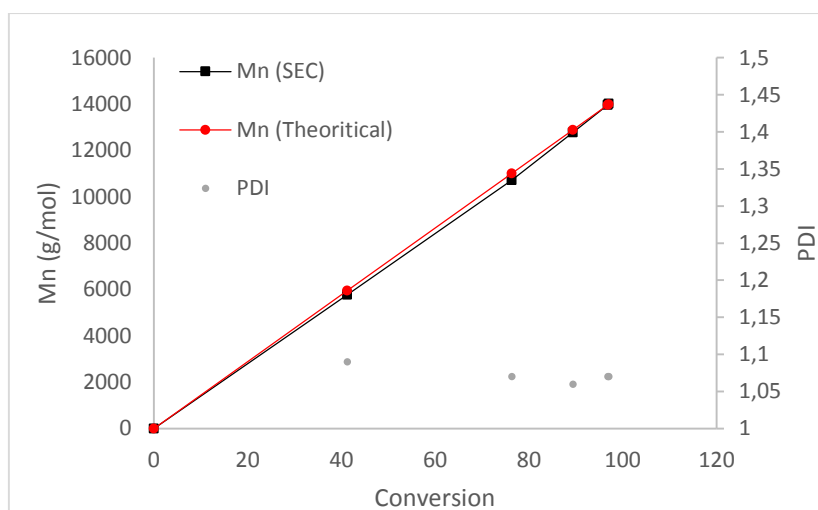


Figure S40: Plot of the molecular weight determined by SEC (■) and the theoretical one (●) vs the conversion for **1** under immortal condition with 1000 equivalents of *rac*-LA and 10 equivalents of IPA. Conditions: [*rac*-LA] = 1M, THF, 25 °C

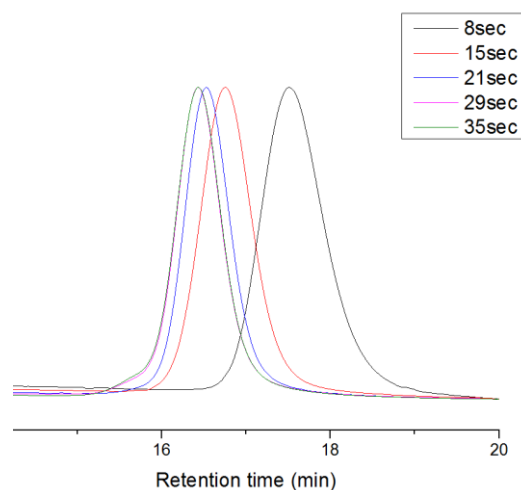


Figure S41: Overlap of SEC traces for **1** during the polymerization of 1000 equivalents of *rac*-LA under immortal condition (10 eq. of IPA). Conditions: [*rac*-LA] = 1M, THF, 25 °C

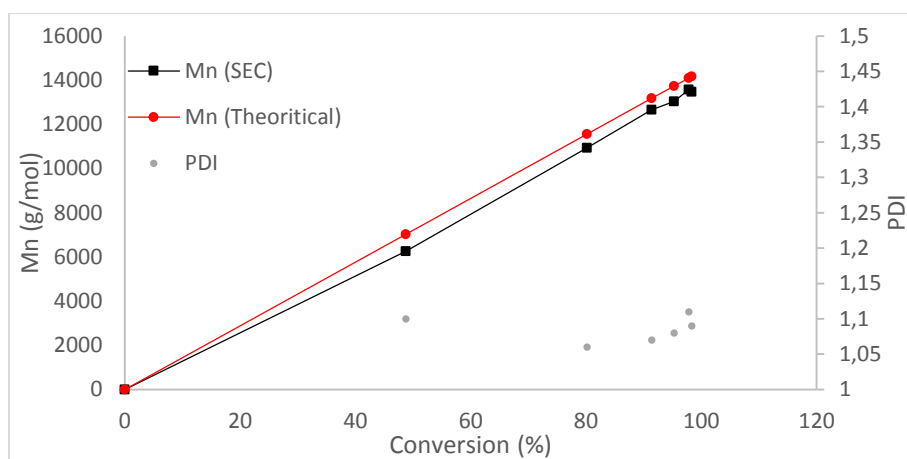


Figure S42: Plot of the molecular weight determined by SEC (■) and the theoretical one (●) vs the conversion for **2** under immortal condition with 1000 equivalents of rac-LA and 10 equivalents of IPA. Conditions: [rac-LA] = 1M, THF, 25 °C

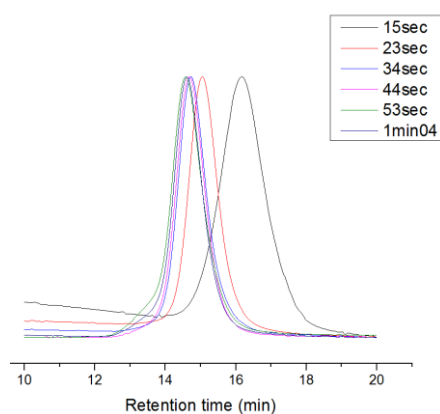


Figure S43: Overlap of SEC traces for **2** during the polymerization of 1000 equivalents of rac-LA under immortal condition (10 eq. of IPA). Conditions: [rac-LA] = 1M, THF, 25 °C

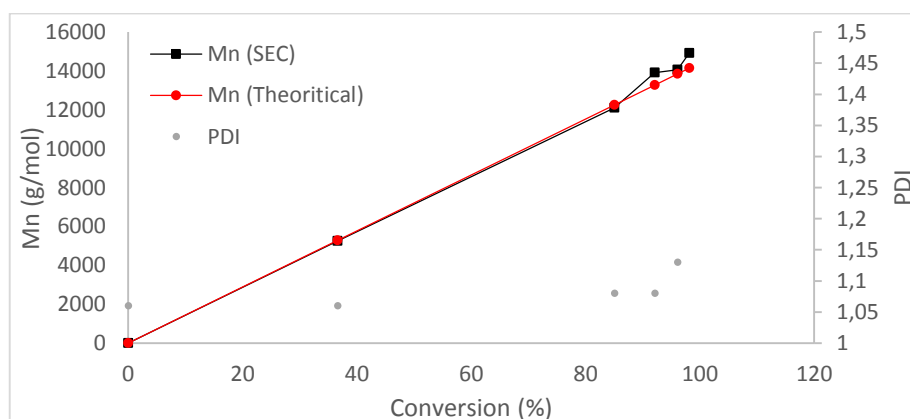


Figure S44: Plot of the molecular weight determined by SEC (■) and the theoretical one (●) vs the conversion for **3** under immortal condition with 1000 equivalents of rac-LA and 10 equivalents of IPA. Conditions: [rac-LA] = 1M, THF, 25 °C

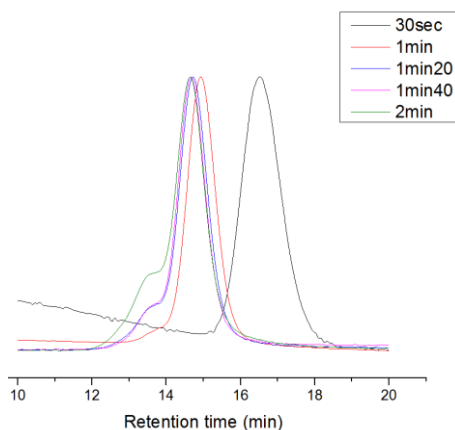


Figure S45: Overlap of SEC traces for **3** during the polymerization of 1000 equivalents of *rac*-LA under immortal condition (10 eq. of IPA). Conditions: [*rac*-LA] = 1M, THF, 25 °C

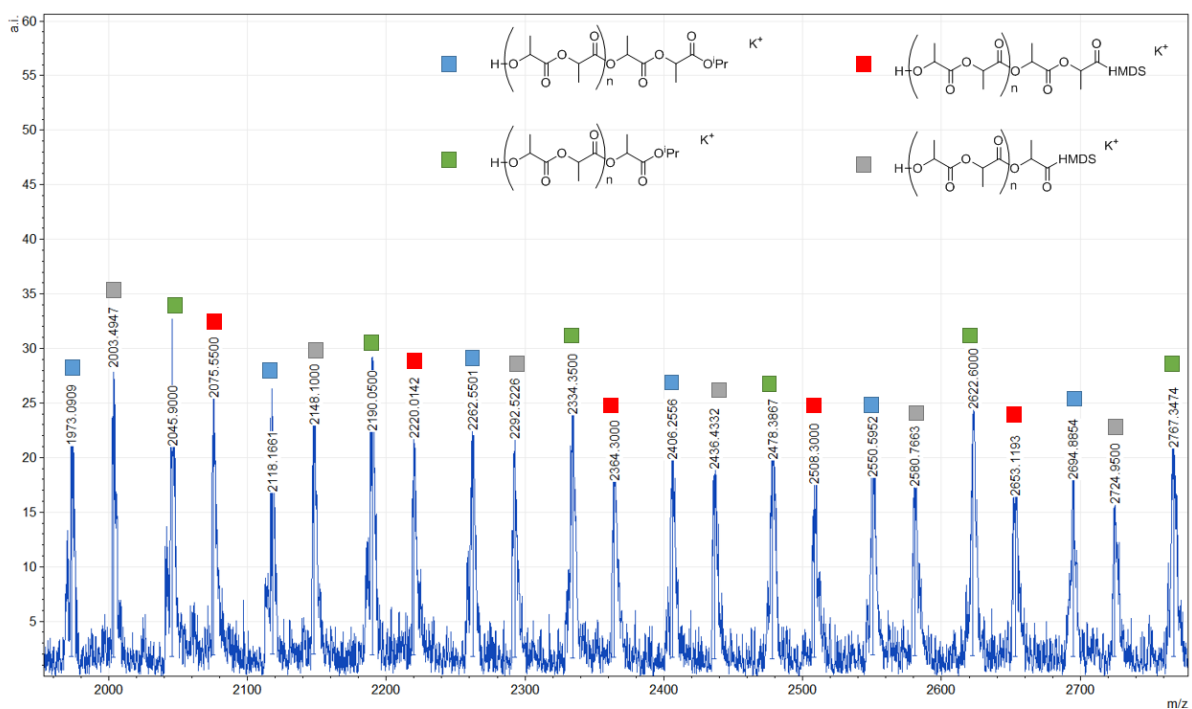


Figure S46: Typical example of a MALDI-ToF spectrum obtained for an immortal polymerization reaction starting from **1**, **2** or **3**. In this case, the polymer was synthesised using **3** at 25 °C in THF with 10 eq. of IPA and 1000eq of *rac*-LA.

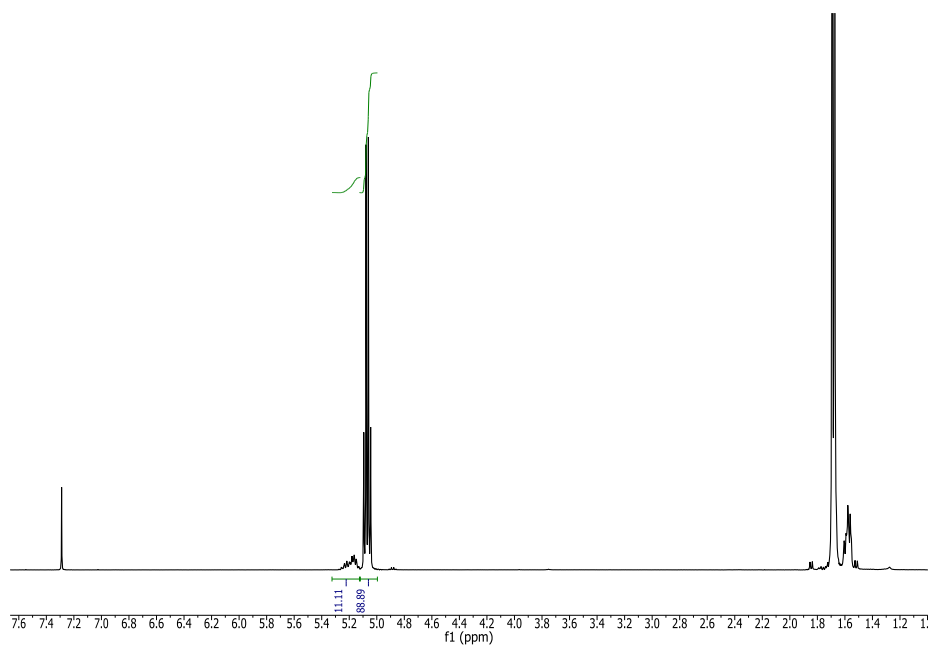


Figure S47: ^1H NMR spectrum corresponding to the entry 1 in table 1; polymerization of 5000 eq. of *rac*-LA using **1**.
 Conditions: $[\text{rac-LA}] = 1\text{M}$, THF, 25 °C

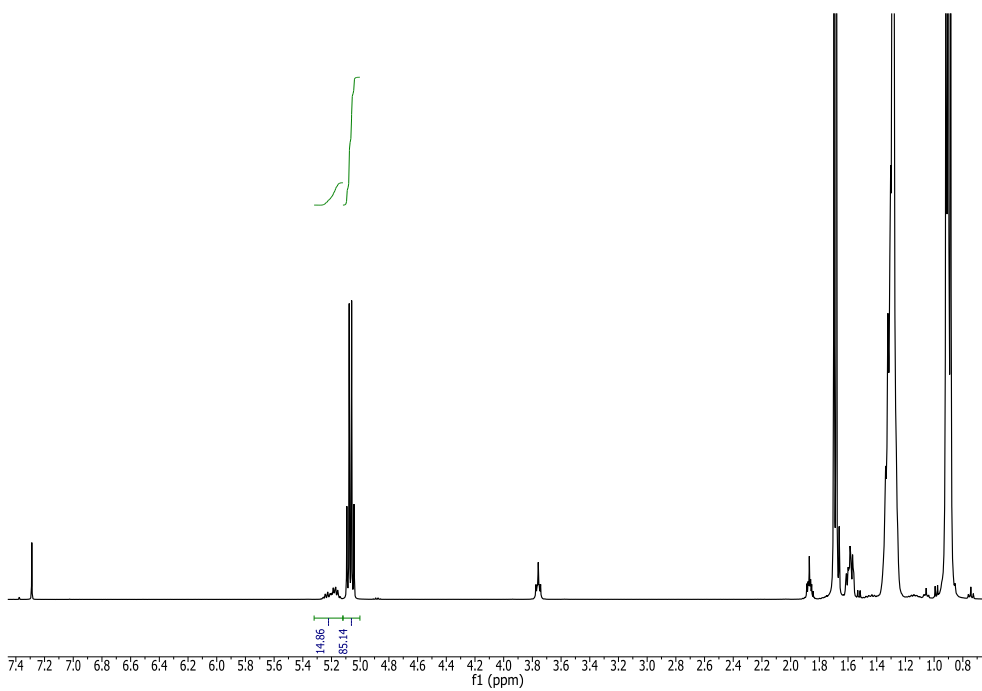


Figure S48: ^1H NMR spectrum corresponding to the entry 2 in table 1; polymerization of 5000 eq. of *rac*-LA using **2**.
 Conditions: $[\text{rac-LA}] = 1\text{M}$, THF, 25 °C

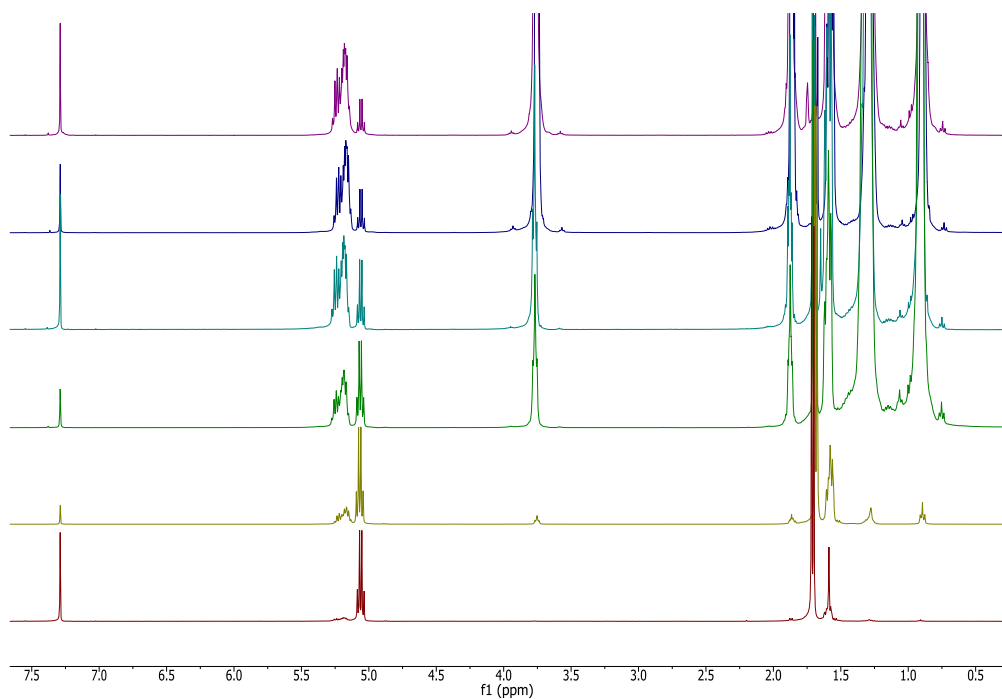


Figure S49: Stack of ¹H NMR spectra for the kinetic study of the polymerization of 5000 eq. of rac-LA using **1** in presence of 10 eq. of IPA. Conditions: [rac-LA] = 1M, THF, 25 °C

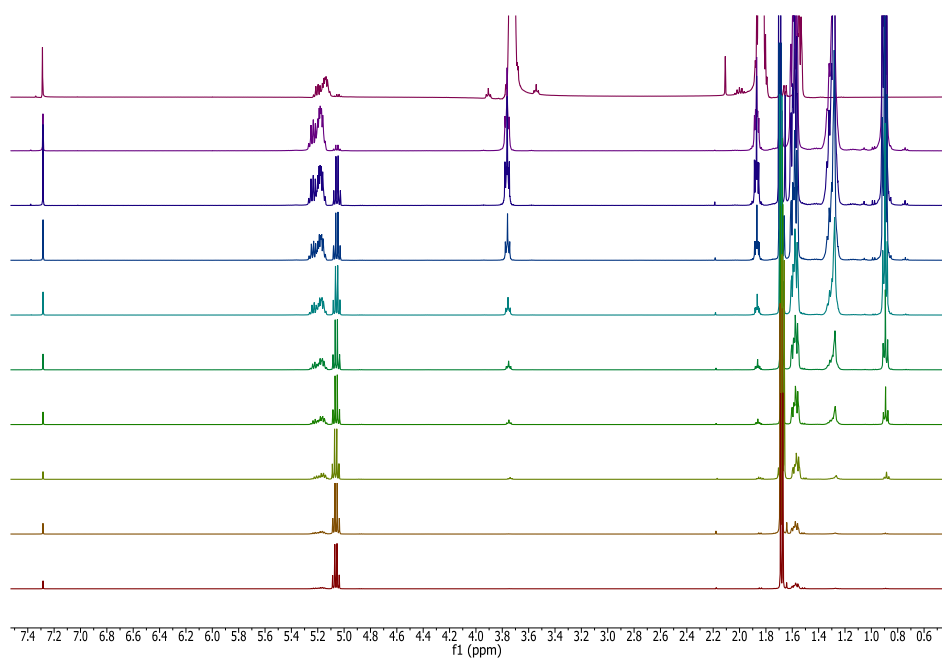


Figure S50: Stack of ¹H NMR spectra for the kinetic study of the polymerization of 5000 eq. of rac-LA using **2** in presence of 10 eq. of IPA. Conditions: [rac-LA] = 1M, THF, 25 °C

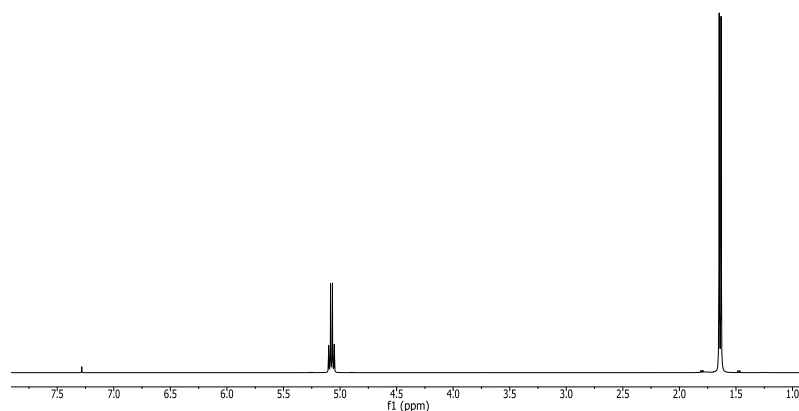


Figure S51: ^1H NMR spectrum corresponding to the entry 5 in table 1; polymerization of 5000 eq. of rac-LA using **3** in presence of 10 eq of IPA. Conditions: $[\text{rac-LA}] = 1\text{M}$, THF, 25 °C

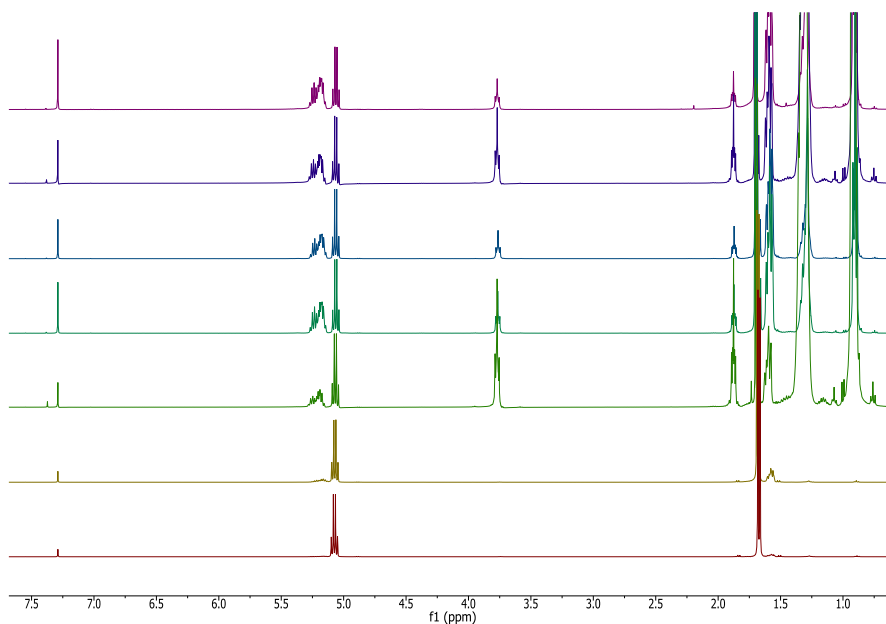


Figure S52: Stack of ^1H NMR spectra for the kinetic study of the polymerization of 10,000 eq. of rac-LA using **1** in presence of 20 eq. of IPA. Conditions: $[\text{rac-LA}] = 1\text{M}$, THF, 25 °C

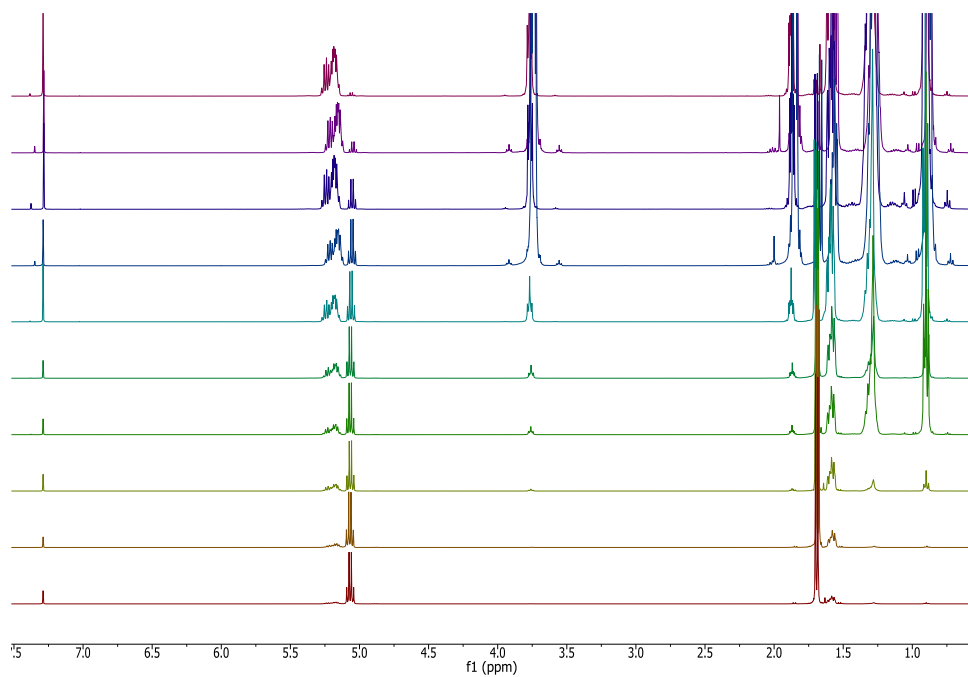


Figure S53: Stack of ^1H NMR spectra for the kinetic study of the polymerization of 10,000 eq. of rac-LA using **2** in presence of 20 eq. of IPA. Conditions: $[\text{rac-LA}] = 1\text{M}$, THF, 25 °C

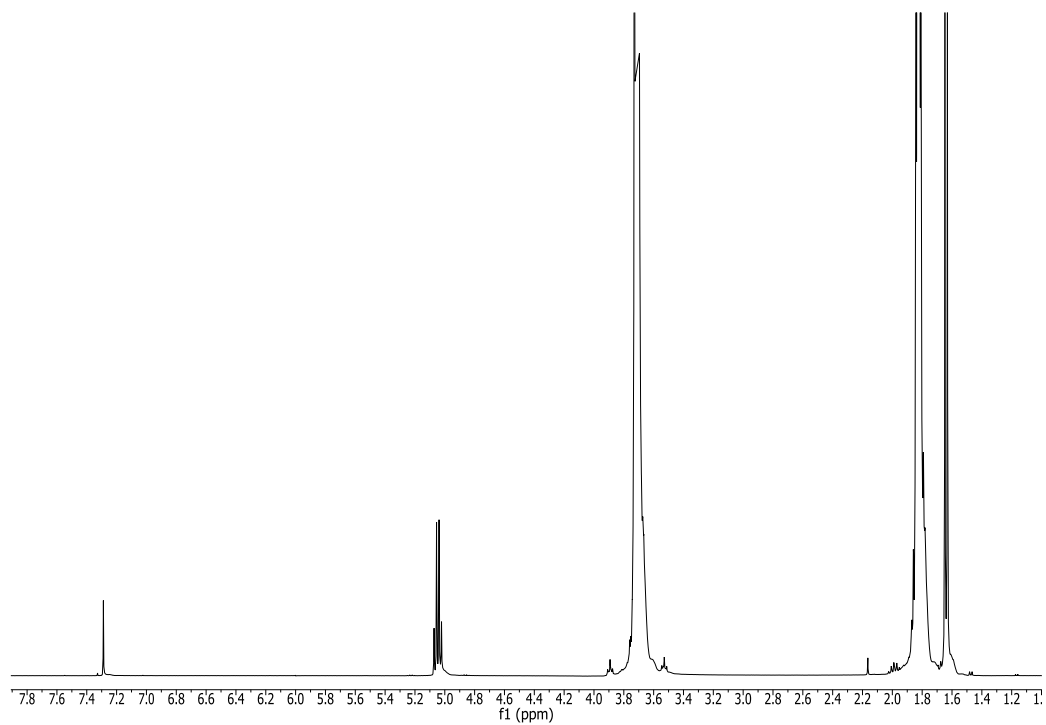


Figure S54: ^1H NMR spectrum corresponding to the entry 8 in table 1; polymerization of 20,000 eq. of rac-LA using **1** in presence of 40 eq. of IPA. Conditions: $[\text{rac-LA}] = 1\text{M}$, THF, 25 °C

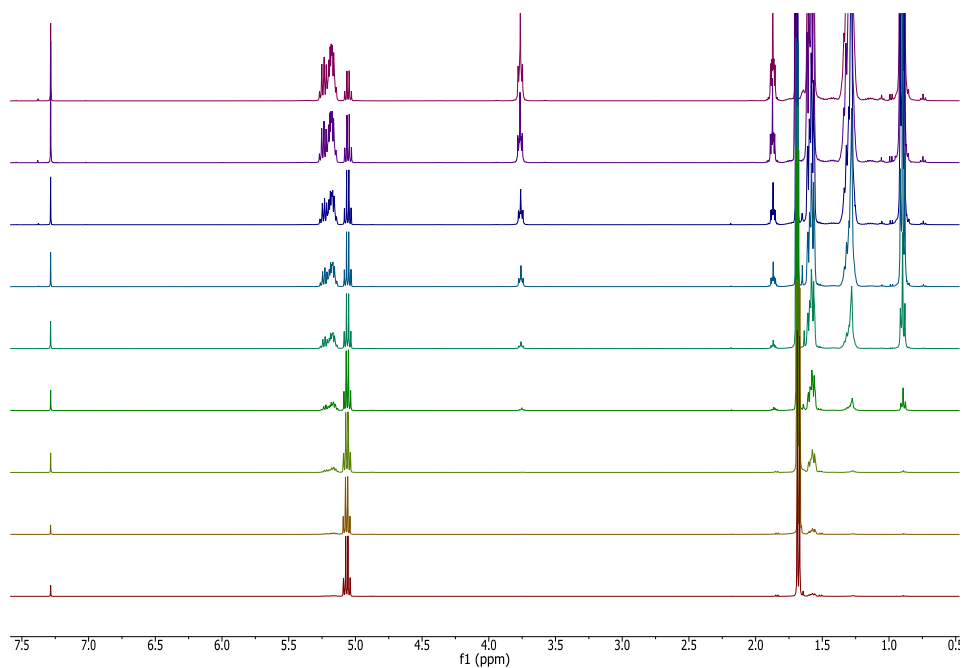


Figure S55: Stack of ¹H NMR spectra for the kinetic study of the polymerization of 20,000 eq. of rac-LA using **2** in presence of 40 eq. of IPA. Conditions: [rac-LA] = 1M, THF, 25 °C.

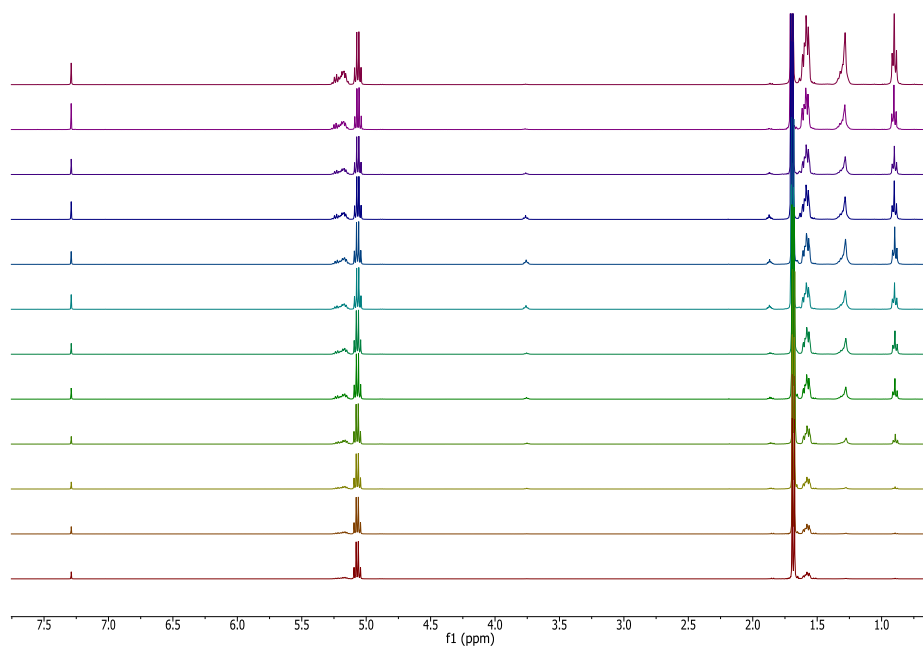


Figure S56: Stack of ¹H NMR spectra for the kinetic study of the polymerization of 50,000 eq. of rac-LA using **2** in presence of 50 eq. of IPA. Conditions: [rac-LA] = 1M, THF, 25 °C.

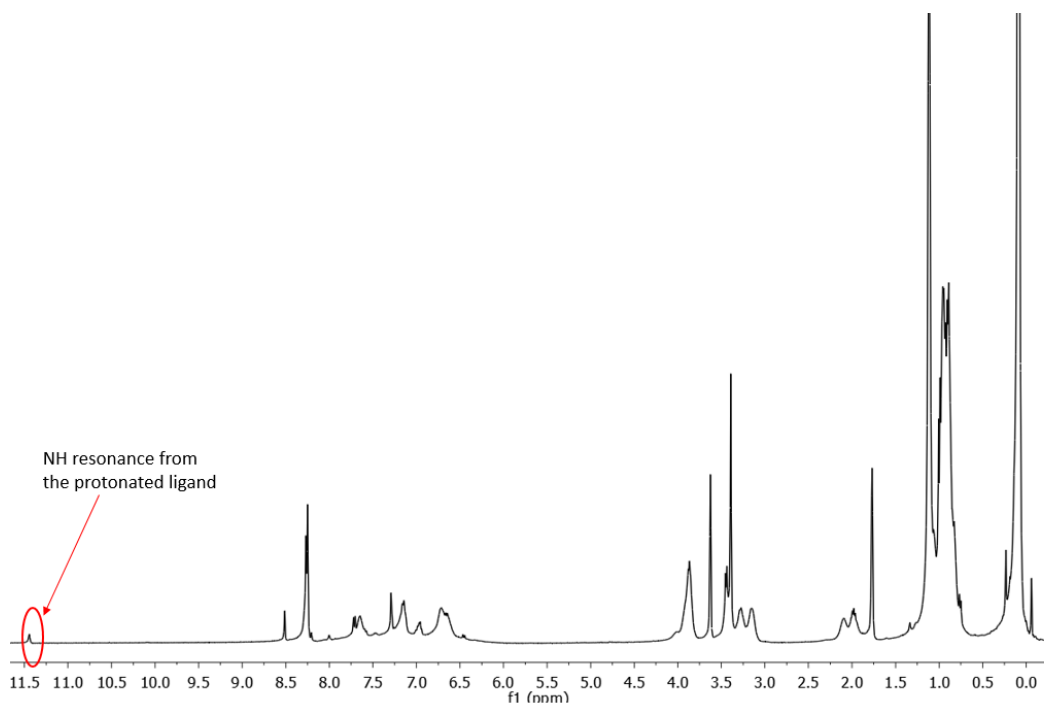


Figure S57: ^1H NMR of **3** (C_6D_6 , 298 K) after 1h of reaction with 2 eq. of IPA

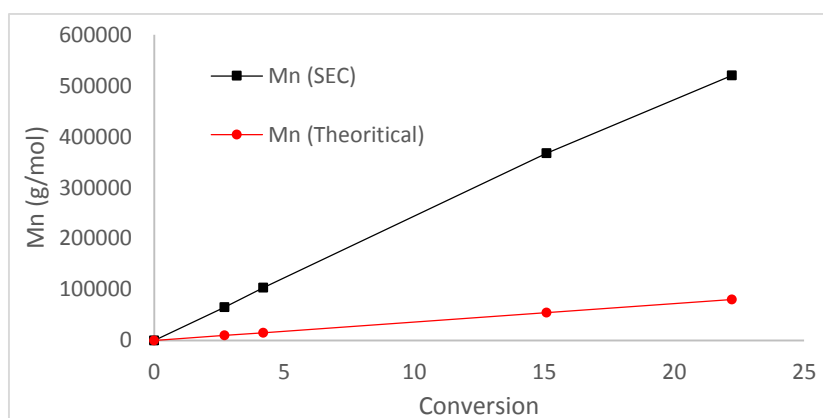


Figure S58: Plot of the molecular weight determined by SEC (■) and the theoretical one (●) vs the conversion for **2** with 5000 equivalents of *rac*-LA. Conditions: [*rac*-LA] = 1M, THF, 25 °C

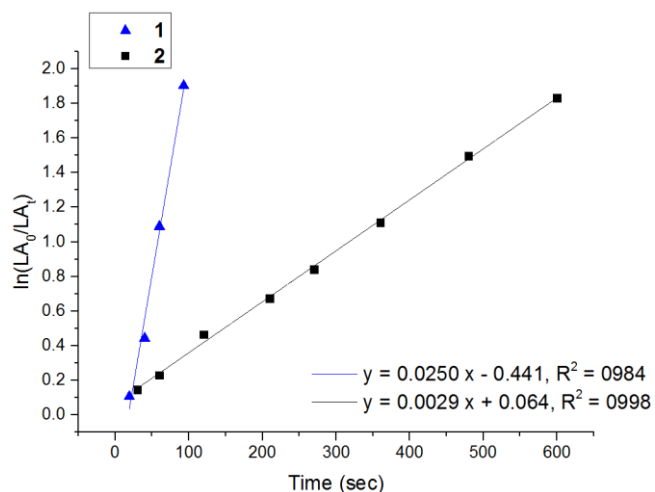


Figure S59: Plot of $\ln([LA]_0/[LA]_t)$ vs time for **1** (▲) and **2** (■) at 25 °C under immortal condition with 5000 equivalents of *rac*-LA and 10 equivalents of IPA. Conditions: [*rac*-LA] = 1M, THF.

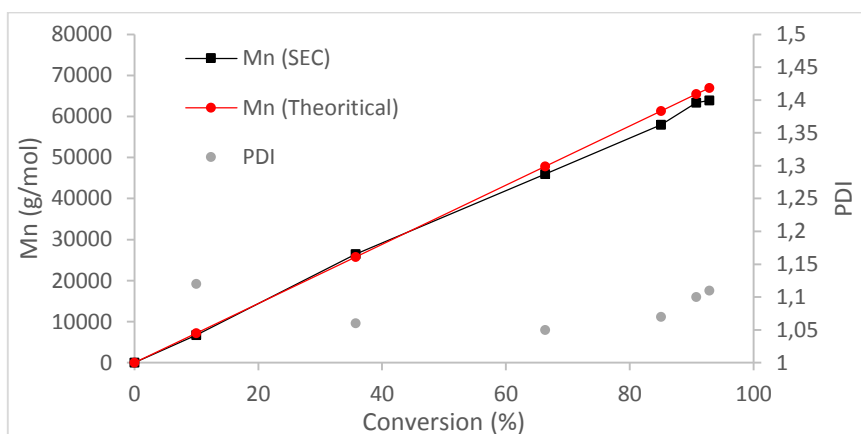


Figure S60: Plot of the molecular weight determined by SEC (■) and the theoretical one (●) vs the conversion for **1** under immortal condition with 5000 equivalents of *rac*-LA and 10 equivalents of IPA. Conditions: [*rac*-LA] = 1M, THF, 25 °C

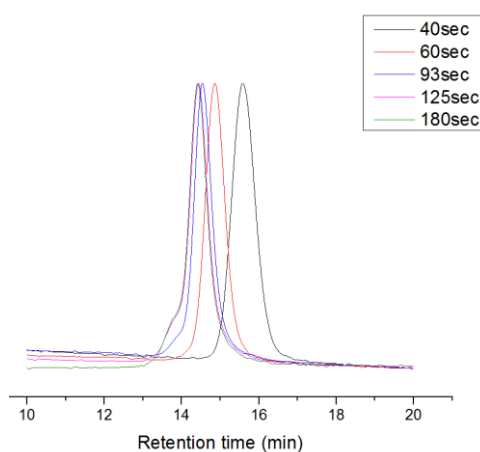


Figure S61: Overlap of SEC traces for **1** during the polymerization of 5000 equivalents of *rac*-LA under immortal condition (10 eq. of IPA). Conditions: [*rac*-LA] = 1M, THF, 25 °C

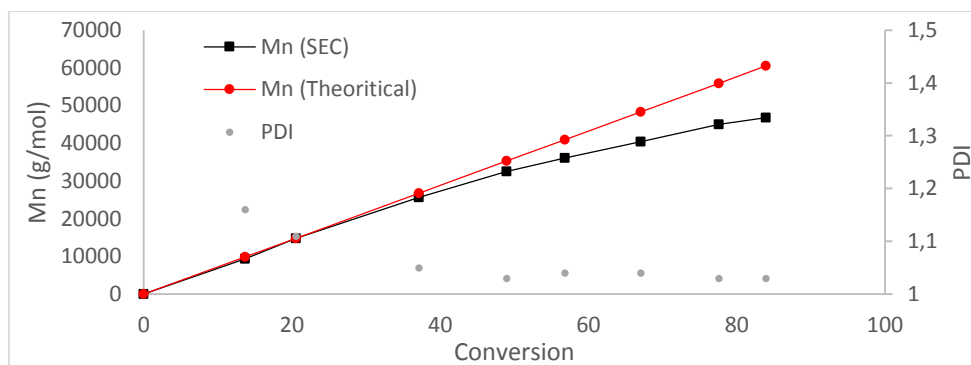


Figure S62: Plot of the molecular weight determined by SEC (■) and the theoretical one (●) vs the conversion for **2** under immortal condition with 5000 equivalents of *rac*-LA and 10 equivalents of IPA. Conditions: [*rac*-LA] = 1M, THF, 25 °C

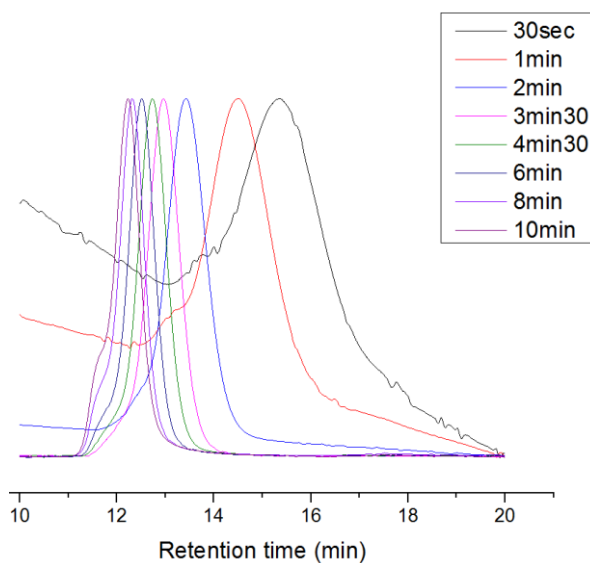


Figure S63: Overlap of SEC traces for **2** during the polymerization of 5000 equivalents of *rac*-LA under immortal condition (10 eq. of IPA). Conditions: [*rac*-LA] = 1M, THF, 25 °C

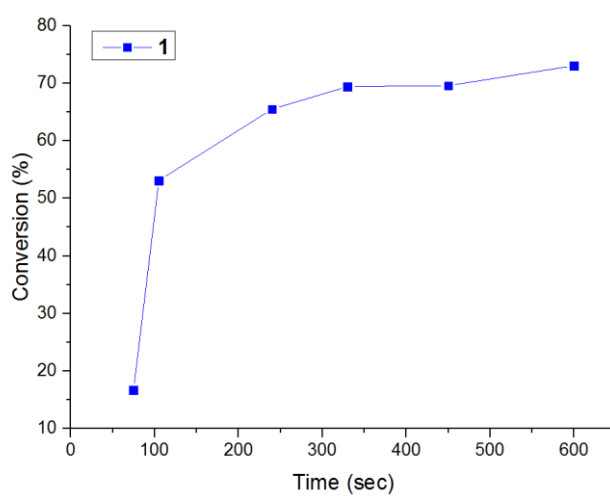


Figure S64: Plot of conversion vs time for **1** (■) at 25 °C under immortal condition with 10,000 equivalents of *rac*-LA and 20 equivalents of IPA. Conditions: [*rac*-LA] = 1M, THF.

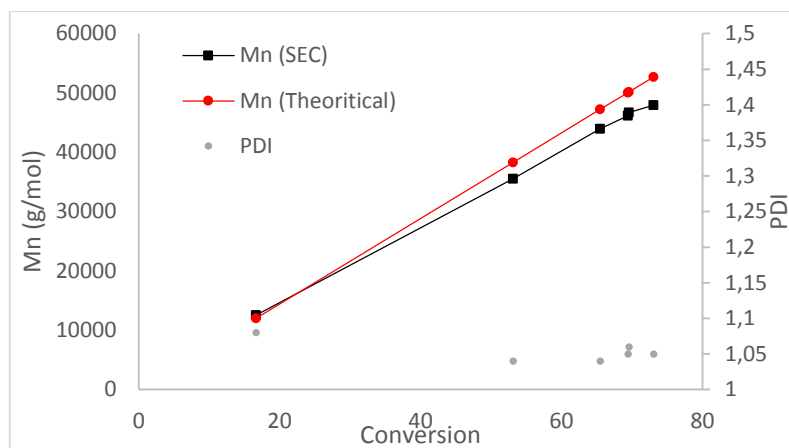


Figure S65: Plot of the molecular weight determined by SEC (■) and the theoretical one (●) vs the conversion for **1** under immortal condition with 10,000 equivalents of *rac*-LA and 20 equivalents of IPA. Conditions: [*rac*-LA] = 1M, THF, 25 °C

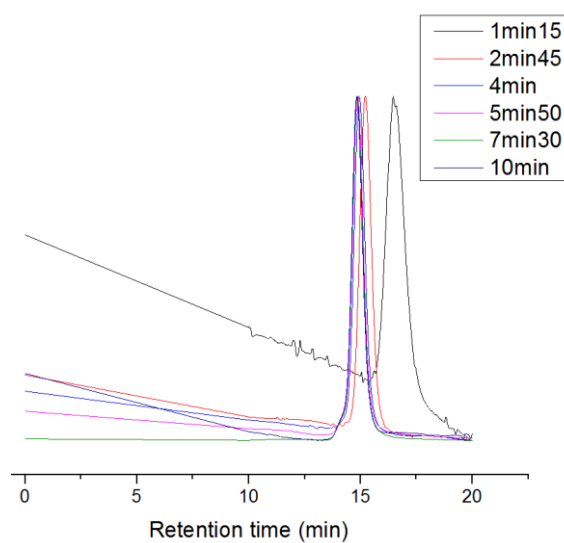


Figure S66: Overlap of SEC traces for **1** during the polymerization of 10000 equivalents of *rac*-LA under immortal condition (20 eq. of IPA). Conditions: [*rac*-LA] = 1M, THF, 25 °C

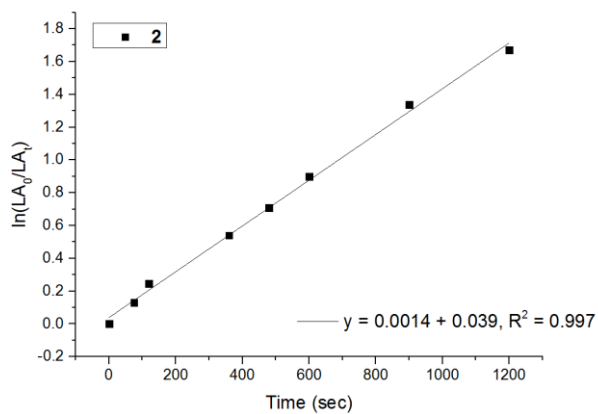


Figure S67: Plot of $\ln([LA]_0/[LA]_t)$ vs time for **2** (■) at 25 °C under immortal condition with 10,000 equivalents of *rac*-LA and 20 equivalents of IPA. Conditions: [*rac*-LA] = 1M, THF.

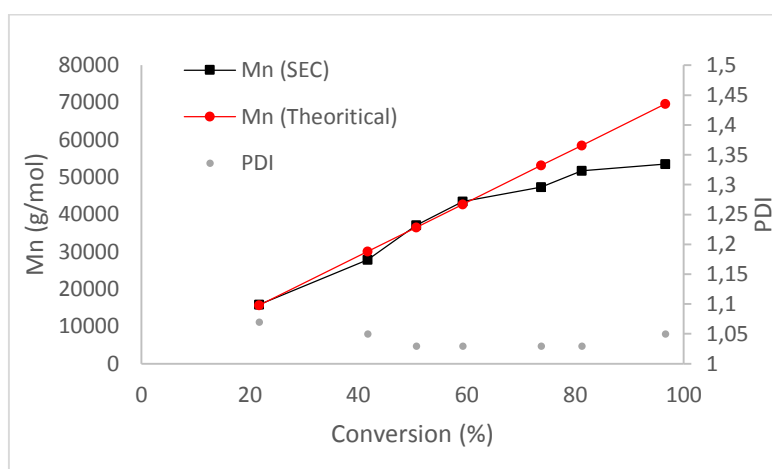


Figure S68: Plot of the molecular weight determined by SEC (■) and the theoretical one (●) vs the conversion for **2** under immortal condition with 10,000 equivalents of *rac*-LA and 20 equivalents of IPA. Conditions: [*rac*-LA] = 1M, THF, 25 °C

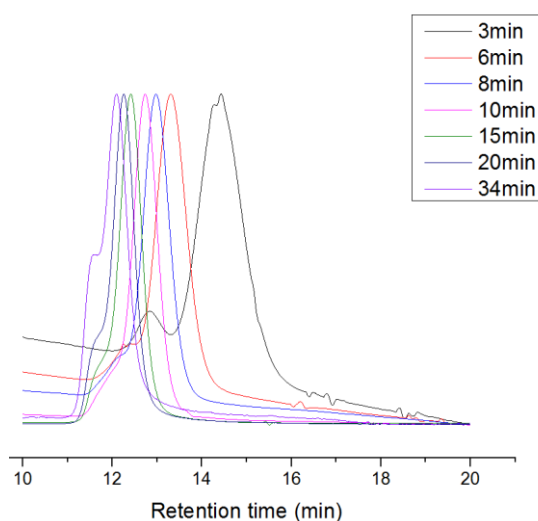


Figure S69: Overlap of SEC traces for **2** during the polymerization of 10000 equivalents of *rac*-LA under immortal condition (20 eq. of IPA). Conditions: [*rac*-LA] = 1M, THF, 25 °C

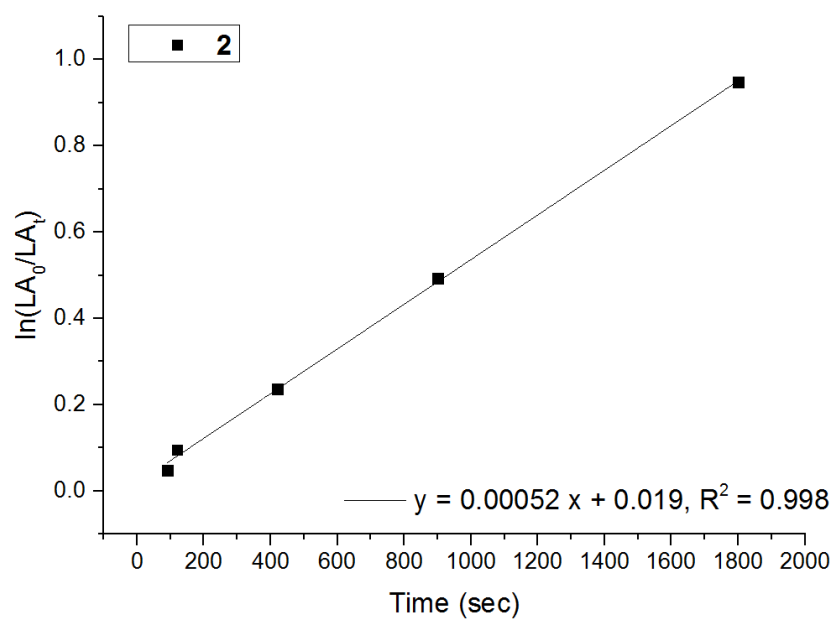


Figure S70: Plot of $\ln([LA]_0/[LA]_t)$ vs time for **2** (■) at 25 °C under immortal condition with 20,000 equivalents of rac-LA and 40 equivalents of IPA. Conditions: [rac-LA] = 1M, THF.

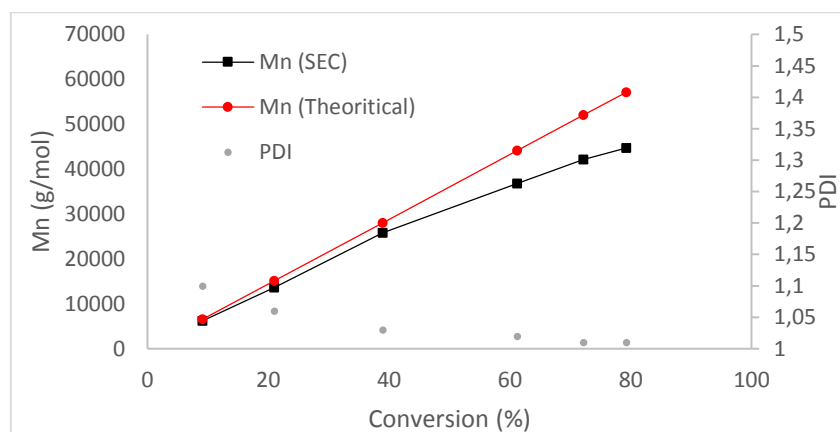


Figure S71: Plot of the molecular weight determined by SEC (■) and the theoretical one (●) vs the conversion for **2** under immortal condition with 20,000 equivalents of rac-LA and 40 equivalents of IPA. Conditions: [rac-LA] = 1M, THF, 25 °C

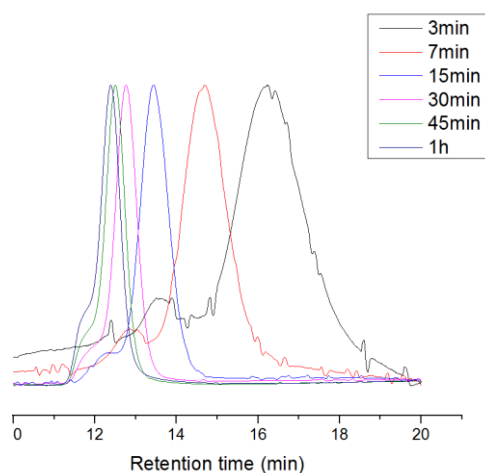


Figure S72: Overlap of SEC traces for **2** during the polymerization of 20000 equivalents of *rac*-LA under immortal condition (40 eq. of IPA). Conditions: [*rac*-LA] = 1M, THF, 25 °C

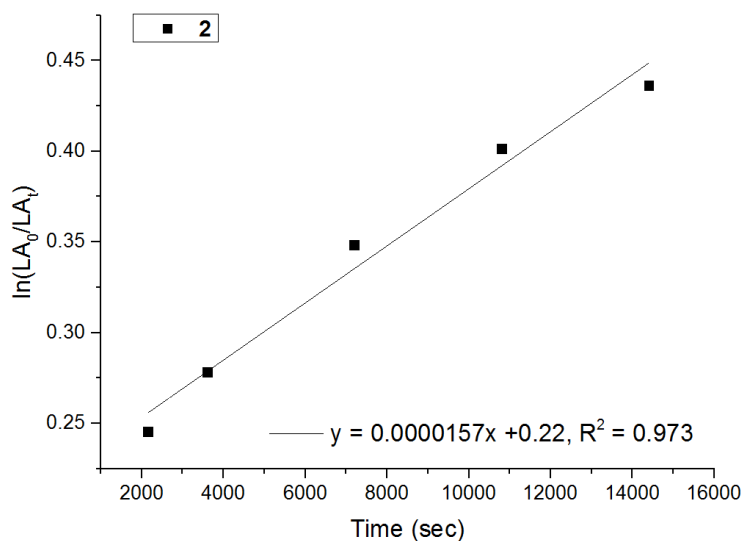


Figure S73: Plot of $\ln([LA_0]/[LA_i])$ vs time for **2** (■) at 25 °C under immortal condition with 50,000 equivalents of *rac*-LA and 50 equivalents of IPA. Conditions: [*rac*-LA] = 1M, THF.

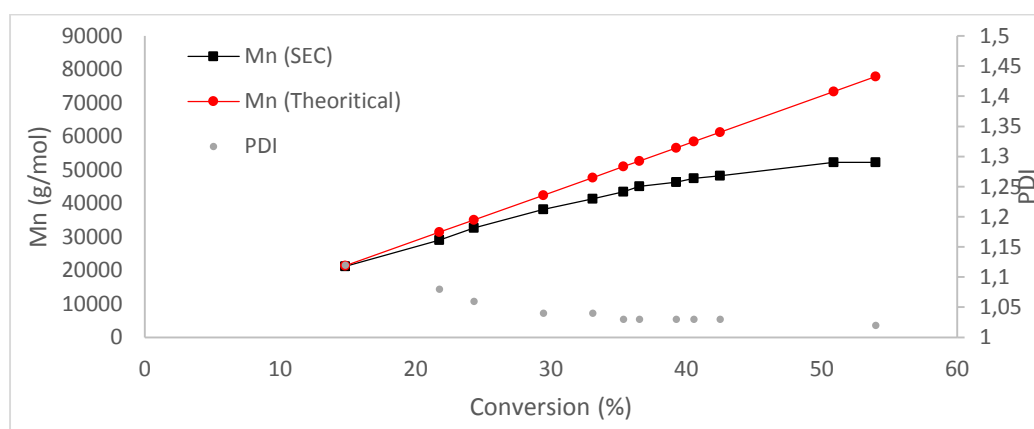


Figure S74: Plot of the molecular weight determined by SEC (■) and the theoretical one (●) vs the conversion for **2** under immortal condition with 50,000 equivalents of *rac*-LA and 50 equivalents of IPA. Conditions: [*rac*-LA] = 1M, THF, 25 °C

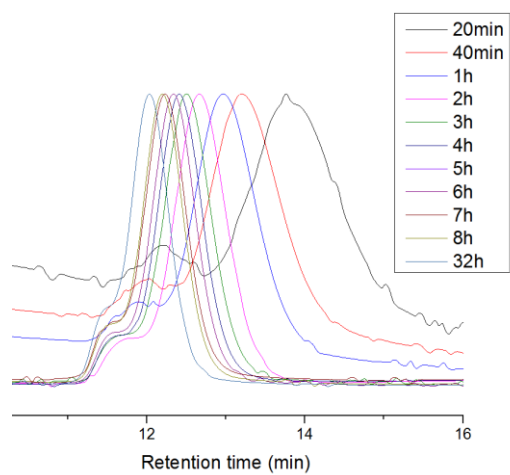


Figure S75: Overlap of SEC traces for **2** during the polymerization of 50000 equivalents of *rac*-LA under immortal condition (50 eq. of IPA). Conditions: [*rac*-LA] = 1M, THF, 25 °C

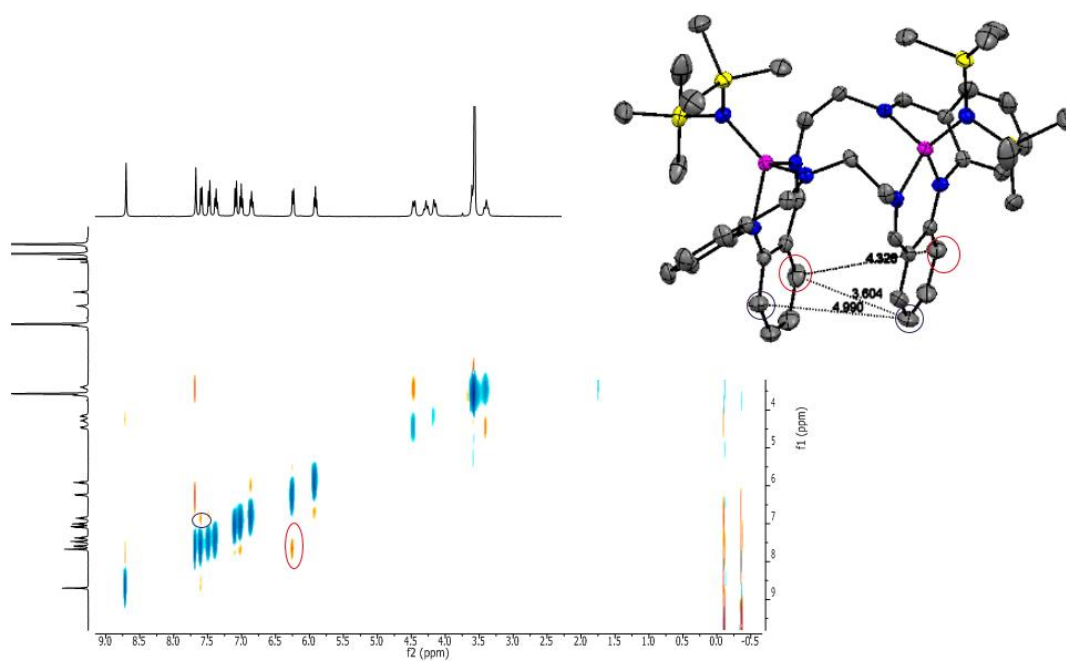


Figure S76: ROZY spectrum of **1** (d_8 -THF, 193 K)

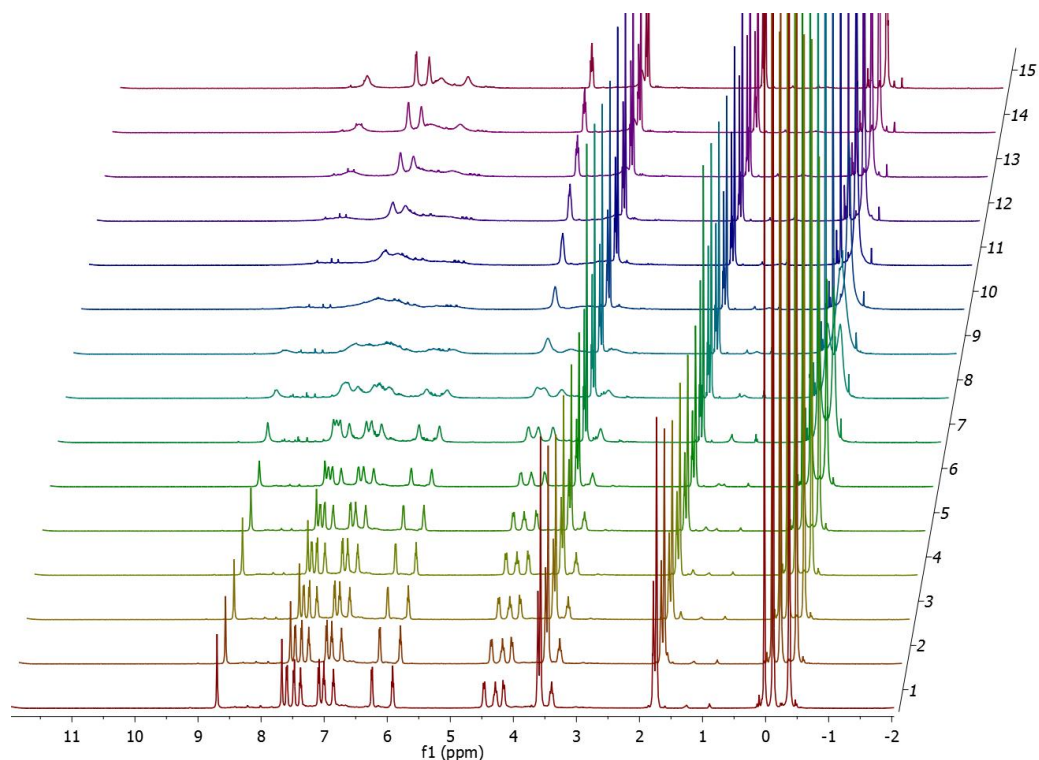


Figure S77: Overlaid of ^1H NMR spectrum of **1** from 193 K (lower) to 333 K (higher) with $\Delta t = 10$ K (d_8 -THF)

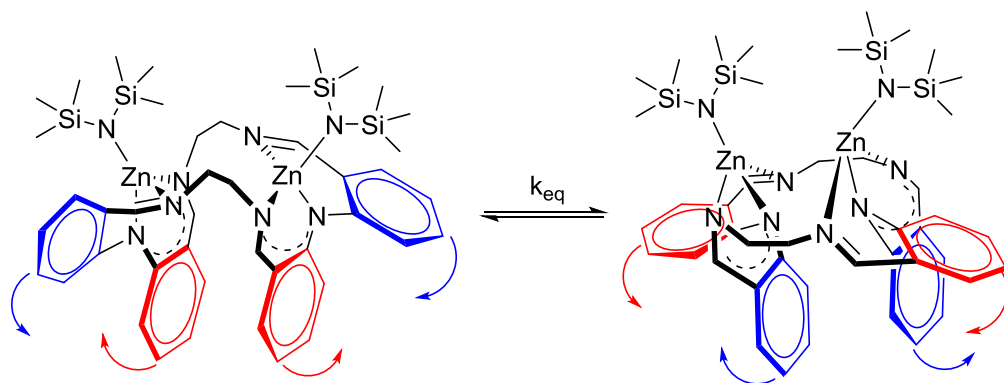


Figure S78: Proposed dynamic process where two folded conformer of **1** are in equilibrium. The rearrangement process is supposed to occur via a rotation of the two phenyl unit around the central nitrogen between them. During this process the BDI chelate flip from one side of the complex to the other side. The folded structure is supposed to be stabilized due to π - π interaction between the two opposite phenyl units. The rotation is therefore supposed to occurs on both side at the same time to maximise this π - π interaction.

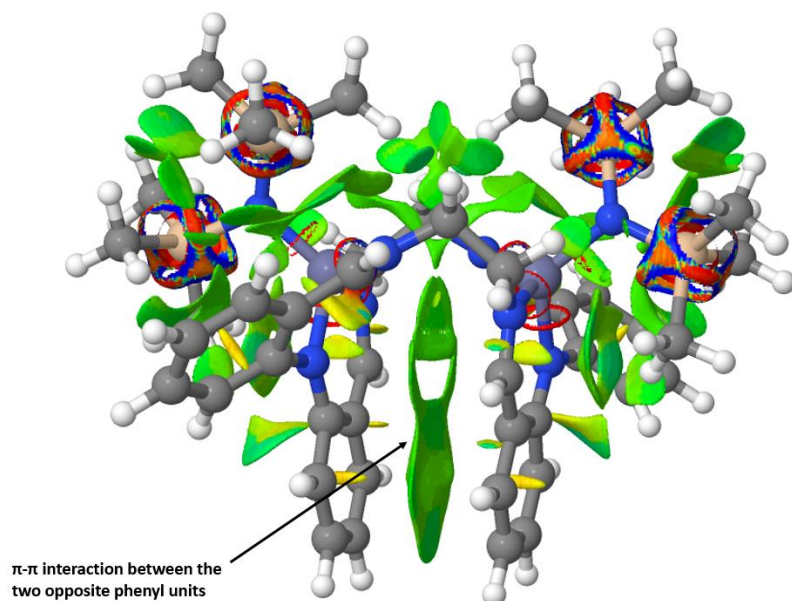


Figure S79: Representation revealing non-covalent interaction surface in **1**. The green colour represent attractive interaction and red colour repulsive interaction. The representation shows the π - π interaction between the two opposite phenyl units.⁵

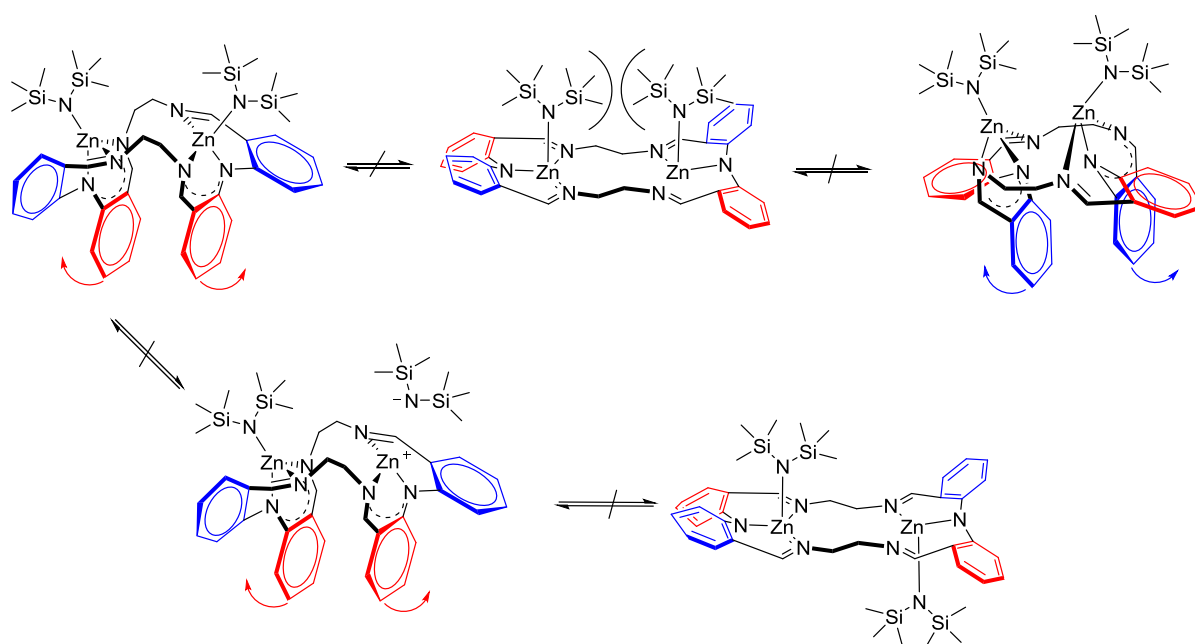


Figure S80: Other less favourable equilibrium. The top route involves the formation of a planar geometry which is not favourable due to the bulkiness of the amido co-ligand and the loss of the π - π interaction between the two opposite phenyl units. The formation of a planar complex **1** as proposed in the second route would involve a dissociative procedure where first the breaking of the Zn-N(TMS)₂ bond occurs, then formation of a planar complex and finally re-coordination of the amido on the opposite face of the complex. The solid state of **1** indicates the Zn-N(TMS)₂ bonds [Zn-N(TMS)₂ = 1.941(2) Å] are larger than other BDI zinc amido complexes [Zn-N(TMS)₂ ≈ 1.890(2) Å] but in the same range as other half salen and imine ligands [Zn-N(TMS)₂ = 1.940 Å]. The dissociation is therefore unfavourable. Again, the formation of such kind of complex would result in a loss of the π - π interaction between the two opposite phenyl units.

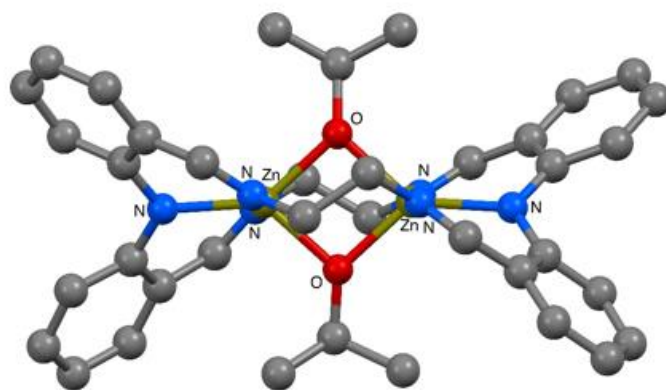


Figure S81: Molecular structure of **4**⁶

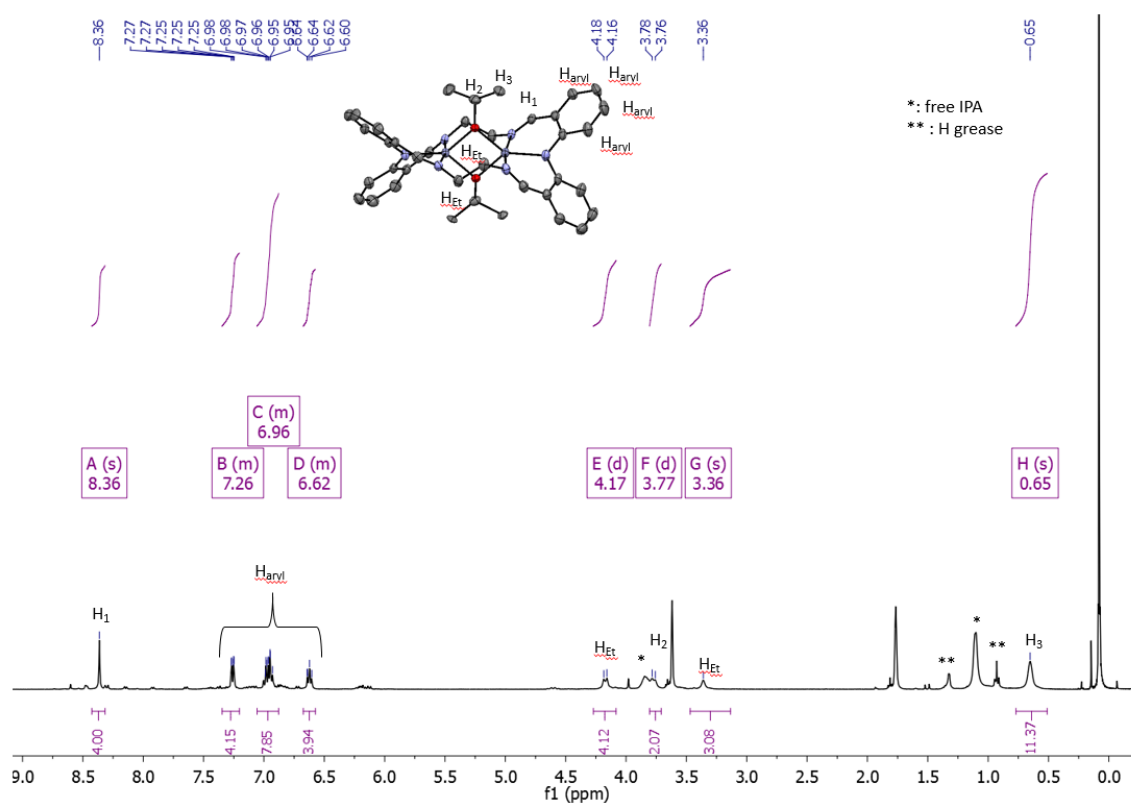


Figure S82: ¹H NMR spectrum of **4** in d₈-THF (T = 298 K).

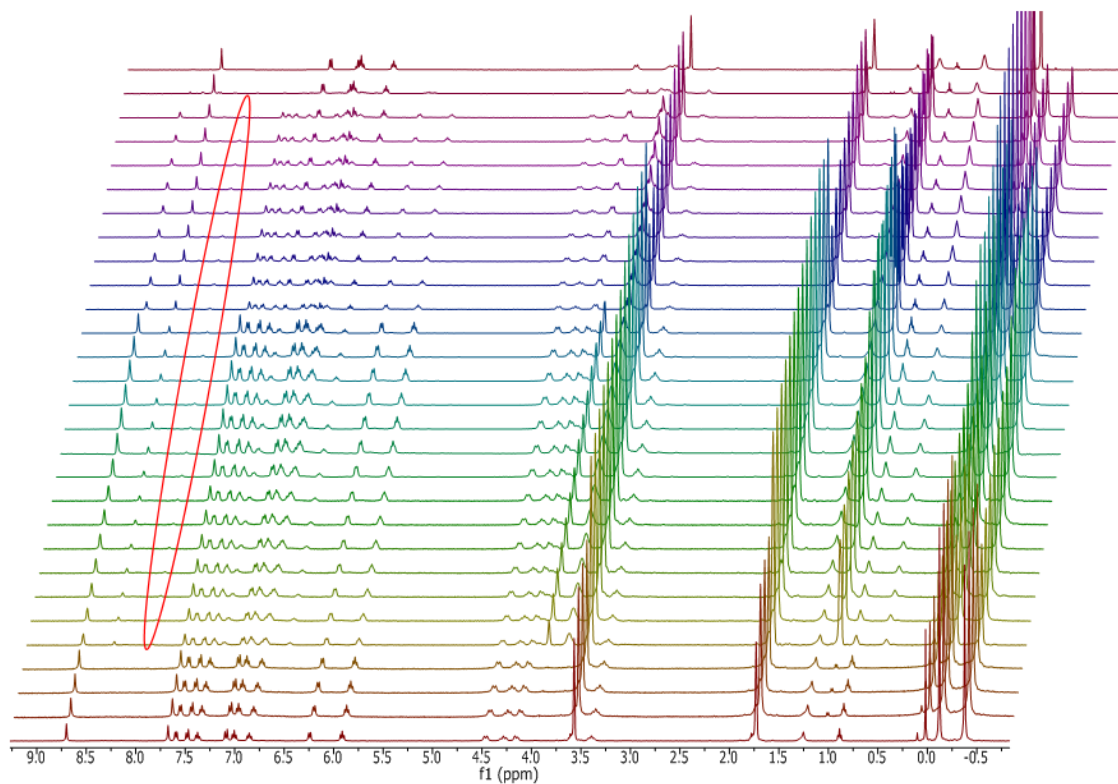


Figure S83: Overlaid of ¹H NMR spectra of the reaction of **1** with two equivalents of IPA in d₈-THF at 183 K. The lower spectrum correspond **1** and the upper one to **4**. The red ellipse show the imine region of the potential intermediate folded alkoxide.

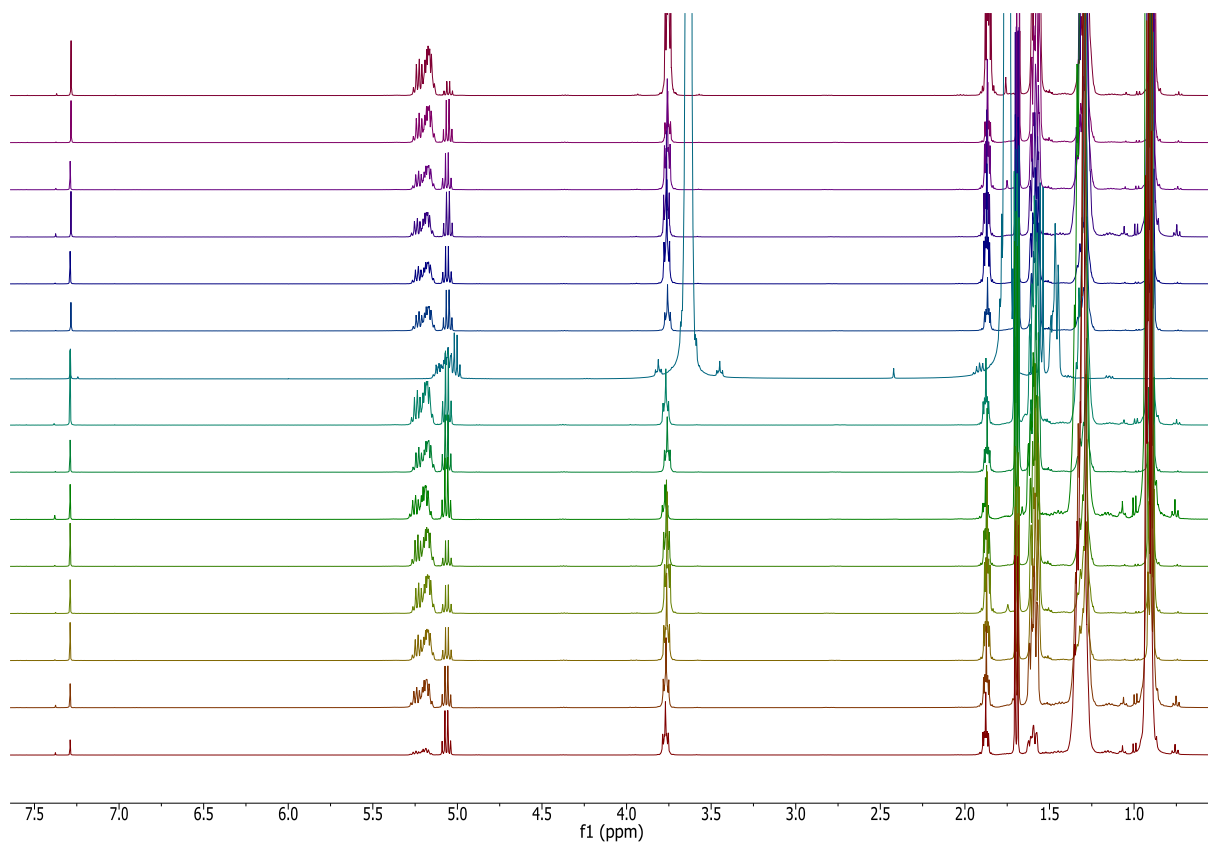


Figure S84: Stack of ^1H NMR spectra for the kinetic study of the polymerization of 1,000 + 200 eq. of rac-LA using **1** in presence of 10 eq. of IPA. Conditions: [rac-LA] = 1M, THF, 25 °C.

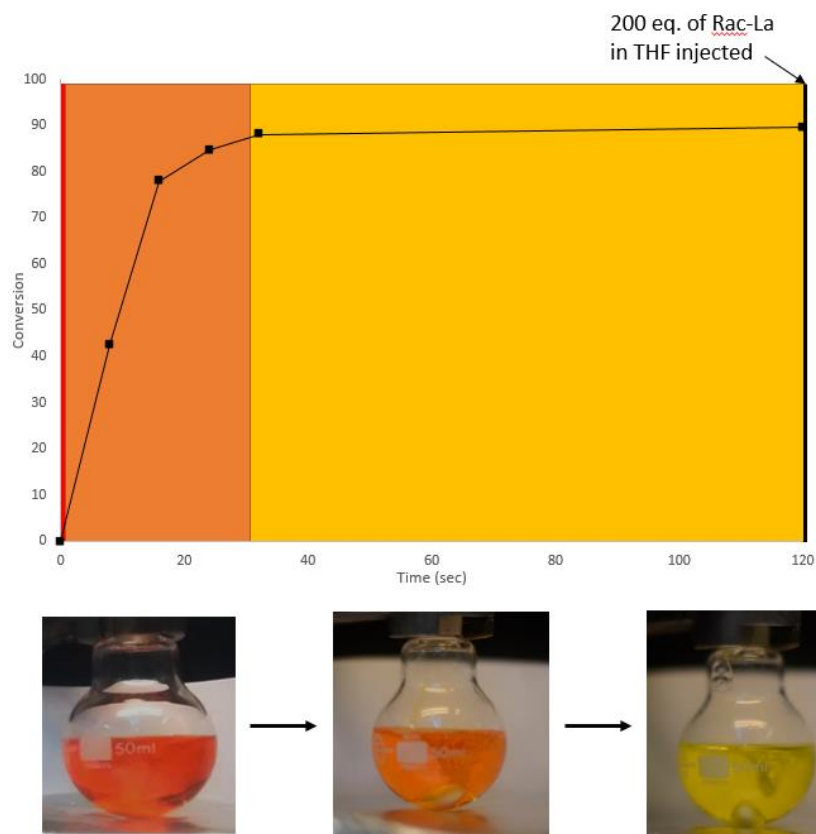


Figure S85: Plot of the conversion of rac-LA vs time for **1** (■) at 25 °C under immortal condition with 1,000 equivalents of rac-LA and 10 equivalents of IPA. Conditions: [rac-LA] = 1M, THF. The coloured rectangle correspond to the colour of the reaction at different times as it is shown by the three pictures underneath the plot.

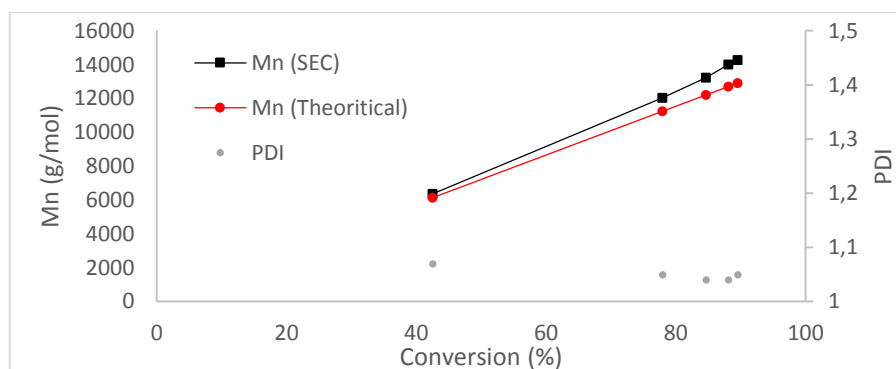


Figure S86: Plot of the molecular weight determined by SEC (■) and the theoretical one (●) vs the conversion for **1** under immortal condition with 1000 equivalents of rac-LA and 10 equivalents of IPA. Conditions: [rac-LA] = 1M, THF, 25 °C

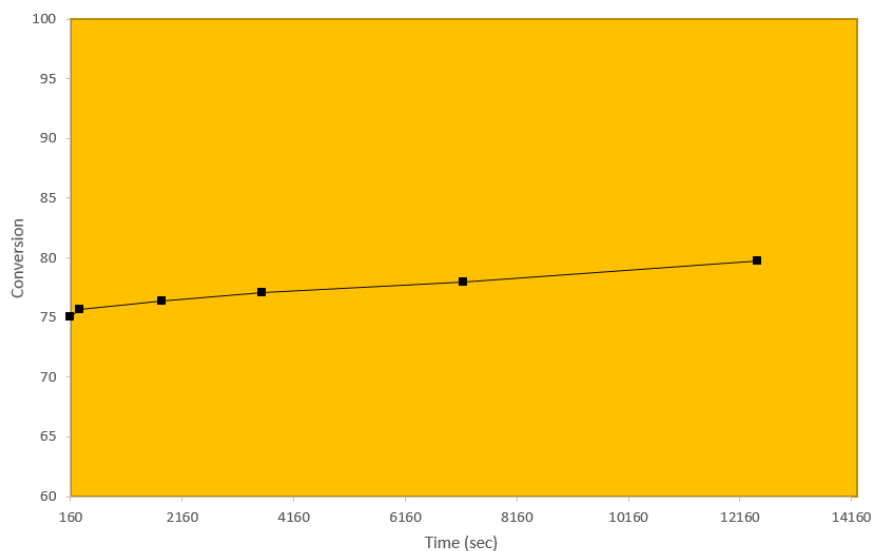


Figure S87: Plot of the conversion of rac-LA vs time for **1** (■) at 25 °C after the addition of 200 eq extra rac-LA monomers to a solution of **1** after full conversion of 1000 eq. of rac-LA. Conditions: [rac-LA] = 1M, THF. The coloured rectangle correspond to the colour of the reaction at different times.

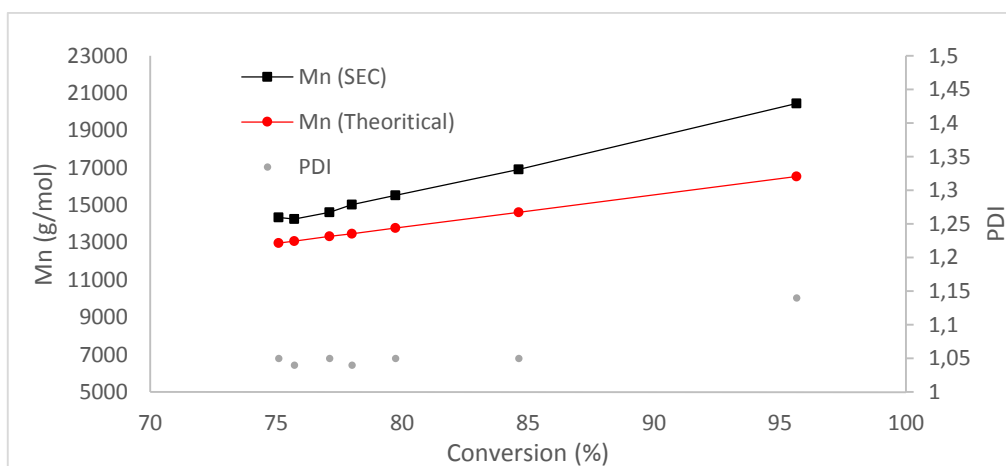


Figure S88: Plot of the molecular weight determined by SEC (■) and the theoretical one (●) vs the conversion for **1** under immortal condition with 1000+200 equivalents of rac-LA and 10 equivalents of IPA. Conditions: [rac-LA] = 1M, THF, 25 °C

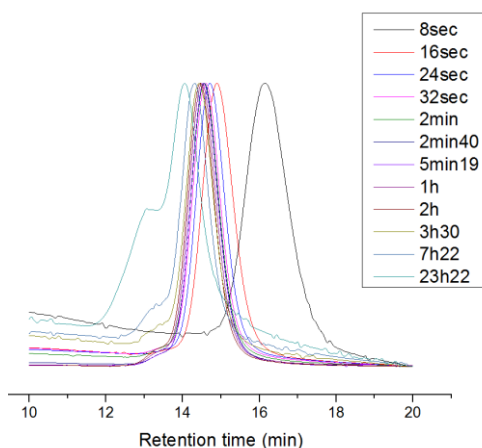


Figure S89: Overlap of SEC traces for **1** during the polymerization of 1000 +200 equivalents of *rac*-LA under immortal condition (10 eq. of IPA). Conditions: [*rac*-LA] = 1M, THF, 25 °C

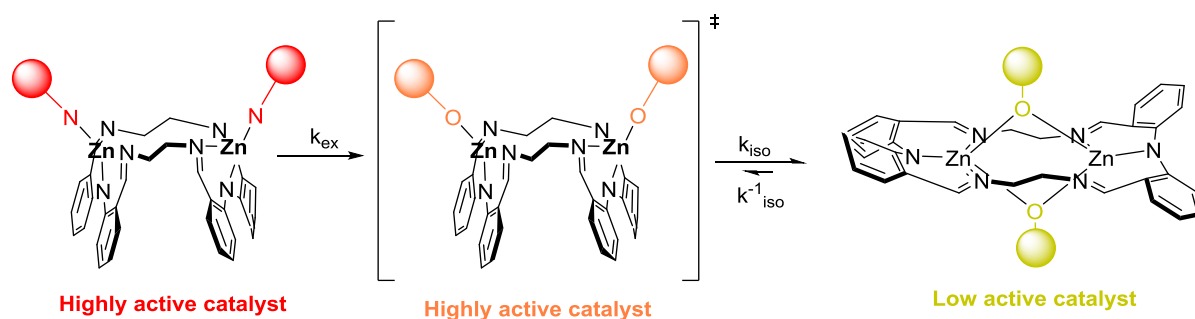


Figure S90: Proposed mechanism for the reaction of two equivalents of IPA on **1**.

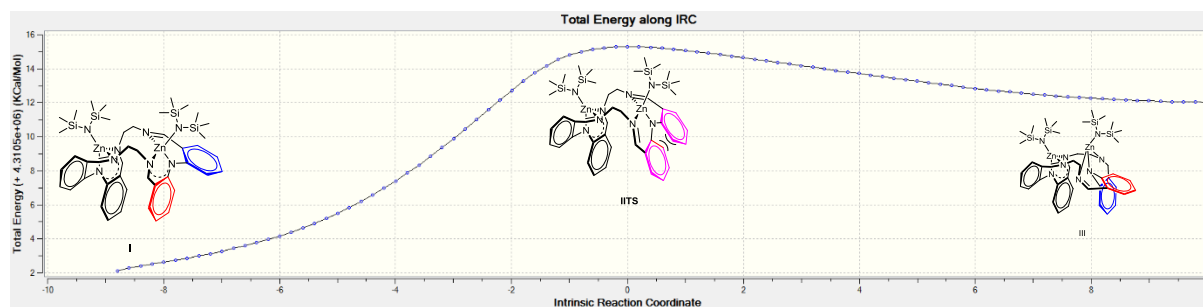


Figure S91: IRC calculations showing interconversion between two aromatic units.

DFT protocol: # IRC=(maxpoints=45,recalc=5,calcfc,maxcycle=40,tight,cartesian,lqa,stepsize=20) rwb97xd/6-31G(d)
scrf=(cpcm,solvent=THF)

Table S2: Data for the DFT calculations as illustrated in Figure S91

Structure	ΔG	JobID	Link
I	0	Opt: 100432 Freq: 100440	https://dx.doi.org/10.6084/m9.figshare.3181294.v1 https://doi.org/10.14469/hpc/426
II-TS	+16.6	Opt: 1003605 Freq: 10003783	https://doi.org/10.14469/hpc/431 https://doi.org/10.14469/hpc/432
III	+13.1	Opt, Freq: 1004206	https://doi.org/10.14469/hpc/433

IRC	JobID: 10010838	https://doi.org/10.14469/hpc/434
DFT protocol: # rwb97xd/6-31G(d) scrf=(ccp, solvent=thf) geom=nocrowd		

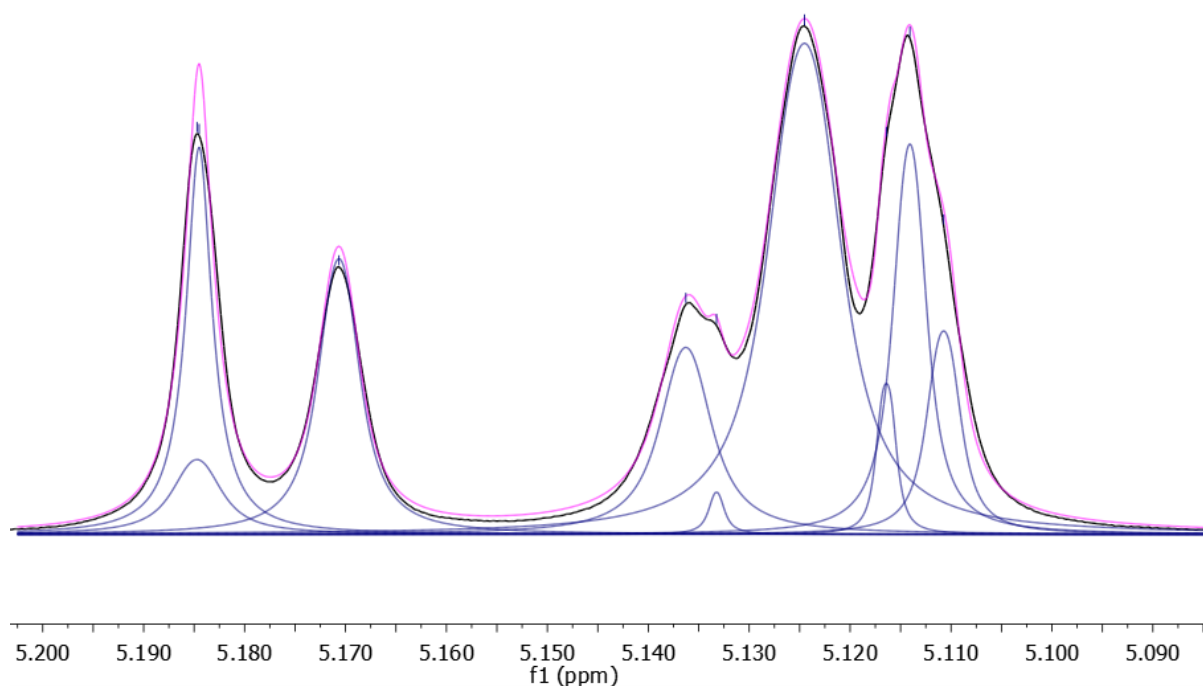


Figure 912: Typical example of a $^1\text{H} \{^1\text{H}\}$ homonuclear decoupled NMR spectrum zoomed in the methyne region of PLA in CDCl_3 at 298 K (in this case, $P_i = 0.54$).

Calculation of the portion of active catalyst in the case HMDS catalysts:

$$\text{Equation S1: } Mn_{exp} = \frac{\text{Conversion} \times Mn_{LA} \times \text{Loading}}{N} \rightarrow \text{Loading} = \frac{N \times Mn_{exp}}{\text{Conversion} \times Mn_{LA}}$$

Mn_{exp} : Mn of the polymer obtained using the SEC Conversion = $\frac{[LA]_t}{[LA]_o}$ $Mn_{LA} = 144.1 \text{ g/mol}$ N = number of initiating groups	Loading for 1 = 7315 Loading for 2 = 2568 Loading for 3 = 1736
---	---

$$\text{Equation S2: } n_{LA} = n_{cat} \times \text{Loading} \rightarrow n_{cat} = \frac{n_{LA}}{\text{Loading}}$$

n_{LA} = number of mmol of lactide used n_{cat} = number of mmol of active catalyst Loading = value calculated previously	<table border="0"> <tr> <td style="padding-right: 10px;">$n_{LA} = 5.3 \text{ mmol (1)}$</td> <td style="padding-right: 10px;">$n_{cat} = 7.2 \times 10^{-4} \text{ mmol (1)}$</td> </tr> <tr> <td style="padding-right: 10px;">$n_{LA} = 5.1 \text{ mmol (2)}$</td> <td style="padding-right: 10px;">$n_{cat} = 2.0 \times 10^{-3} \text{ mmol (2)}$</td> </tr> <tr> <td style="padding-right: 10px;">$n_{LA} = 8.9 \text{ mmol (3)}$</td> <td style="padding-right: 10px;">$n_{cat} = 5.1 \times 10^{-4} \text{ mmol (3)}$</td> </tr> </table>	$n_{LA} = 5.3 \text{ mmol (1)}$	$n_{cat} = 7.2 \times 10^{-4} \text{ mmol (1)}$	$n_{LA} = 5.1 \text{ mmol (2)}$	$n_{cat} = 2.0 \times 10^{-3} \text{ mmol (2)}$	$n_{LA} = 8.9 \text{ mmol (3)}$	$n_{cat} = 5.1 \times 10^{-4} \text{ mmol (3)}$
$n_{LA} = 5.3 \text{ mmol (1)}$	$n_{cat} = 7.2 \times 10^{-4} \text{ mmol (1)}$						
$n_{LA} = 5.1 \text{ mmol (2)}$	$n_{cat} = 2.0 \times 10^{-3} \text{ mmol (2)}$						
$n_{LA} = 8.9 \text{ mmol (3)}$	$n_{cat} = 5.1 \times 10^{-4} \text{ mmol (3)}$						

$$\text{Equation S3: } \%_{\text{active cat}} = \frac{n_{cat}}{n_{cato}}$$

$\%_{active\ cat}$ = percentage of active catalyst	$n_{LA} = 5.3 \times 10^{-3}$ mmol (1)	$\%_{active\ cat} = 14\%$
n_{cat} = determined previously	$n_{LA} = 5.1 \times 10^{-3}$ mmol (2)	$\%_{active\ cat} = 40\%$
n_{cat0} = number of mmol of catalyst added	$n_{LA} = 8.9 \times 10^{-3}$ mmol (3)	$\%_{active\ cat} = 64\%$

References

1. Bochmann, M.; Bwembya, G.; Webb, K. J.; Malik, M. A.; Walsh, J. R.; O'Brien, P., Arene Chalcogenolato Complexes of Zinc and Cadmium. In *Inorg. Synth.*, John Wiley & Sons, Inc.: 2007; pp 19-24.
2. Cameron, S. A.; Brooker, S., *Inorg. Chem.* **2011**, *50* (8), 3697-3706.
3. (a) Black, D.; Rothnie, N., *Aust. J. Chem.* **1983**, *36* (12), 2395-2406; (b) C. Black, D. S.; Rothnie, N. E., *Tetrahedron Lett.* **1978**, *19* (31), 2835-2836.
4. Kowalski, A.; Duda, A.; Penczek, S., *Macromolecules* **1998**, *31* (7), 2114-2122.
5. Johnson, E. R.; Keinan, S.; Mori-Sánchez, P.; Contreras-García, J.; Cohen, A. J.; Yang, W., *J. Am. Chem. Soc.* **2010**, *132* (18), 6498-6506.
6. Romain, C.; Bennington, M. S.; White, A. J. P.; Williams, C. K.; Brooker, S., *Inorg. Chem.* **2015**, (54), 11842-11851.
7. SHELXTL, Bruker AXS, Madison, WI; (b) SHELX-2013, <http://shelx.uni-ac.gwdg.de/SHELX/index.php>
8. B. M. Chamberlain, M. Cheng, D. R. Moore, T. M. Ovitt, E. B. Lobkovsky, G. W. Coates, *J. Am. Chem. Soc.* **2001**, *123*, 3229-3238.
9. C. K. Williams, L. E. Breyfogle, S. K. Choi, W. Nam, V. G. Young, M. A. Hillmyer, W. B. Tolman, *J. Am. Chem. Soc.* **2003**, *125*, 11350-11359.
10. V. Poirier, T. Roisnel, J.-F. Carpentier, Y. Sarazin, *Dalton Trans.* **2009**, 9820-9827.
11. A. J. Nijenhuis, D. W. Grijpma, A. J. Pennings, *Macromolecules* **1992**, *25*, 6419-6424.